The transverse energy-energy correlator at next-to-next-to-next-to-leading logarithm

Published for SISSA by Springer

Received: *February 12, 2024*
Revised: *July 16, 2024*
Accepted: *September 1, 2024*
Published: *September 13, 2024*

The transverse energy-energy correlator at next-to-next-to-next-to-leading logarithm

Anjie Gao,[a] **Hai Tao Li**,[b] **Ian Moult**[c] **and Hua Xing Zhu**[d,e]

[a]*Center for Theoretical Physics, Massachusetts Institute of Technology, Cambridge, MA 02139, U.S.A.*
[b]*School of Physics, Shandong University, Jinan, Shandong 250100, China*
[c]*Department of Physics, Yale University, New Haven, CT 06511, U.S.A.*
[d]*School of Physics, Peking University, Beijing, 100871, China*
[e]*Center for High Energy Physics, Peking University, Beijing 100871, China*

E-mail: anjiegao@mit.edu, haitao.li@sdu.edu.cn, ian.moult@yale.edu, zhuhx@pku.edu.cn

Abstract: We present an operator based factorization formula for the transverse energy-energy correlator in the back-to-back (dijet) region, and uncover its remarkable perturbative simplicity and relation to transverse momentum dynamics. This simplicity enables us to achieve next-to-next-to-next-to leading logarithmic (N^3LL) accuracy for a hadron collider dijet event shape for the first time. Our factorization formula applies to $W/Z/\gamma$ + jet, and dijet production, providing a natural generalization of transverse momentum observables to one- and two-jet final states. This provides a laboratory for precision studies of QCD and transverse momentum dynamics at hadron colliders, as well as an opportunity for understanding factorization and its violation in a perturbatively well controlled setting.

Keywords: Effective Field Theories of QCD, Factorization, Renormalization Group, Resummation

ArXiv ePrint: 2312.16408

https://doi.org/10.1007/JHEP09(2024)072

JHEP09(2024)072

Contents

1 Introduction

Hadron colliders provide a rich environment for studying Quantum Chromodynamics (QCD). Of particular interest are observables that are amenable to first principles perturbative calculations, of which inclusive event shapes are some of the most well known examples. A large number of event shape variables have been precisely measured at the LHC (see e.g. [1–9]), and have been used for applications ranging from extracting the value of the strong coupling constant [9], to deriving constraints on potential new colored particles [10, 11].

JHEP09(2024)072

Due to remarkable theoretical progress, dijet event shapes in e^+e^- colliders are now under excellent theoretical control, with state-of-the-art predictions incorporating next-to-next-to-next-to-leading logarithmic ($\mathrm{N^3LL}$) [12–15] or $\mathrm{N^4LL}$ resummation [16] of singular contributions, next-to-next-to-leading order (NNLO) fixed order calculations [17–22], and non-perturbative power corrections [13, 23–36]. However, event shapes at hadron colliders are much less well understood. This is due not only to their increased perturbative complexity, but also due to a lack of understanding of the applicability of factorization. In particular, it is known that Glauber effects invalidate standard factorization formulas [37–54], both through spectator interactions, and through the invalidation of collinear factorization for spacelike splittings with multiple colored collinear Wilson lines [55]. Alternatively, this makes precision measurements and high order calculations of hadron collider event shapes of significant interest for understanding a variety of aspects related to QCD factorization.

For hadron collider event shapes, there has been spectacular recent progress on the fixed order side, with the NNLO calculation of hadron collider event shapes [56]. However, there has been much less progress in the study of resummation and factorization for hadron collider event shapes. Next-to-leading logarithmic (NLL) resummation has been achieved for a large number of observables [57, 58]. Next-to-next-to-leading logarithmic (NNLL) resummation has only been achieved for zero-jet [59–61], and one-jet event shapes [62]. $\mathrm{N^3LL}$ resummation was recently achieved for one-jettiness [63]. However, the most interesting dynamics occurs when there are multiple incoming and outgoing colored particles, which first occurs for dijet event shapes. Due to the simultaneous complexity of the color flow and the observables typically considered, relatively little progress has been made in extending resummed calculations for dijet event shapes to higher perturbative orders. However, these observables are interesting both practically, as well as theoretically, for studying the generic structure of factorization theorems.

In this paper we uncover the perturbative simplicity of the transverse energy-energy correlator (TEEC) dijet event shape observable and exploit this to achieve an unprecedented $\mathrm{N^3LL}$ accuracy for a hadron collider dijet event shape, extending the NNLL results presented in [64], and describing some additional aspects of the calculation. While the TEEC has been measured at the LHC [6, 7, 9] (we note that this measurement is on jets instead of hadrons) and used to extract α_s, it has received relatively little theoretical attention (see, however, an NLO calculation of the TEEC for jets [65] and the recent remarkable NNLO calculation [56].). For an interesting recent application of the TEEC to the study of saturation at the future EIC, see [66–69]. On the other hand, the energy-energy correlator (EEC) e^+e^- event shape has recently received significant theoretical attention, including analytic fixed order calculation at NLO [70–72] in QCD, and to NNLO in $\mathcal{N} = 4$ [73–76], a factorization and derivation of the singular structure in the back-to-back limit [77, 78], an understanding of the all orders structure in the collinear limit [79–83], numerical calculations and extractions of α_s [22, 84], and a fixed order calculation of the three-point correlator in the collinear limit [85] and at general angles [86, 87]. They have also been applied in a wide range of phenomenological applications from high energy to nuclear physics [88–99]. We will illustrate how many of these nice features carry over to the back-to-back limit in the hadron collider case.

JHEP09(2024)072

In this paper we derive an operator based factorization formula for the TEEC in the back-to-back (dijet) region, which was first presented without derivation in [64]. This factorization is derived using soft collinear effective theory (SCET) [100–103], and takes a remarkably simple form, being essentially a projection of transverse momentum factorization onto a scattering plane. In particular, the factorization formula involves the standard transverse momentum dependent (TMD) beam functions, as well as the TMD fragmentation functions, making it interesting for studying TMD dynamics. We describe the structure of the renormalization group evolution, give all ingredients required to achieve N^{3}LL resummation, and present numerical results.

Our calculation incorporates a large number of the most precisely known perturbative ingredients in QCD, namely the:

- Three loop quadrupole soft anomalous dimension [104, 105],
- Three loop rapidity anomalous dimension [106],
- Four loop cusp anomalous dimension [107–110],
- NNLO TMD PDFs [111–116],
- NNLO TMD Fragmentation functions [113, 115, 116],
- NNLO TEEC Soft function [64],
- NNLO $2 \to 2$ scattering amplitudes [117–124],

which illustrates the remarkable power of factorization, as well as the complexity of event shapes in a hadron collider environment.

Since the publication of our original result for the TEEC [64], there has been significant progress in perturbative calculations at hadron colliders, in particular the calculation of $2 \to 3$ jet cross section [125] and hadron collider event shapes [56] at NNLO (building on significant progress in the understanding of the properties of $2 \to 3$ amplitudes at NNLO, see e.g. [126–137]). This result provides the necessary order to match to our resummed N^{3}LL result. Additionally, many of the perturbative ingredients necessary to extend the factorization to higher orders have appeared. These included the N^{3}LO TMD PDFs and fragmentation functions [138–141], the four loop rapidity anomalous dimension [16, 142], and the $2 \to 2$ scattering amplitudes at three loops [143–146]. We therefore believe that it is timely to discuss the higher order structure of hadron collider event shapes.

In addition to its direct phenomenological relevance, we believe that the TEEC provides a particularly clean laboratory for studying factorization violation and rapidity factorization at high perturbative orders. For the purposes of studying factorization violation, we also highlight a particularly interesting feature of the TEEC, namely that it can be defined not only for dijet production, but also for $W/Z/\gamma$+jet events by demanding that one of the energy correlators lies on the $W/Z/\gamma$, as well as for Drell-Yan with the γ/Z decaying to leptons, where both correlators are placed on the leptons. Using the results of this paper, the TEEC in all these different final states can be computed at N^{3}LL. We believe that by having the same observable, but with distinct final states, at this level of perturbative accuracy, one

JHEP09(2024)072

can perform a detailed study of color flow and factorization violation. In particular, it is known that the TEEC will factorize for the Drell-Yan process (where it is related to the q_T observable which factorizes [147–153]), while for the dijet process, it is known that it will not factorize. For $W/Z/\gamma$, the status is unclear. In this sense, we can view the TEEC as a generalization of q_T to final state jets. We hope that this will enable advances in the understanding of QCD in hadronic collisions.

An outline of this paper is as follows. In section 2 we define the TEEC and describe its relation to the more familiar EEC observable. In section 3 we discuss the kinematics of the TEEC in the back-to-back limit, and derive the factorization formula describing this limit. We also briefly discuss factorization violation and the effect of underlying event. In section 4 we discuss in detail the soft function appearing in the description of the TEEC in the back-to-back limit, which is the primary new perturbative ingredient required for the TEEC. In section 5 we present a solution to the color space matrix renormalization group equations for the soft function. In section 6 we discuss linearly polarized beam and jet functions that first contribute at N^{3}LL. In section 7 we verify the singular structure predicted by the factorization formula by comparing with a numerical calculation using the NLO three jet cross section. We also make predictions for the singular behavior of the three jet cross section at NNLO. In section 8 we present resummed results for the TEEC at NNLL and N^{3}LL. We conclude in section 9.

2 The transverse energy-energy correlator

In this section we define the TEEC, comparing its definition to the more standard EEC. We also provide definitions of the TEEC which are applicable to color singlet production, and for $W/Z/\gamma+$ jet production. We believe that the ability to compute the observable at N^{3}LL for three distinct final states, with different color flows will provide an important handle in the study of QCD event shape that has not been available previously.

The EEC in e^+e^- is defined as [154–157]

$$\frac{d\sigma}{d\cos\chi} = \sum_X \int d\sigma_{e^+e^-\to X} \sum_{a,b\in X} \frac{E_a E_b}{Q^2} \delta(\cos(\theta_{ab}) - \cos(\chi)) \,, \tag{2.1}$$

where X is the hadronic final state, and a, b sum over the final state hadrons including $a = b$. It measures the flow of energy in two calorimeters separated by an angle χ, as shown in figure 1(a).

The TEEC is the natural extension of the EEC to a hadron collider, and measures the flow of energy in two calorimeters separated by an angle ϕ in the plane transverse to the beam axis as shown in figure 1(b). It is defined as [158]

$$\frac{d\sigma}{d\cos\phi} = \sum_X \int d\sigma_{pp\to X} \sum_{a,b\in X} \frac{E_{T,a} E_{T,b}}{|\sum_{i\in X} E_{T,i}|^2} \delta(\cos\phi_{ab} - \cos\phi) \,, \tag{2.2}$$

with transverse energy $E_T = \sqrt{p_T^2 + m^2}$ for a particle with invariant mass m and transverse momentum p_T. Much like the EEC, the TEEC exhibits singularities at the two extremes of its phase space, which must be resummed to all orders. Much like the EEC, at $\phi = \pi$ we have

JHEP09(2024)072

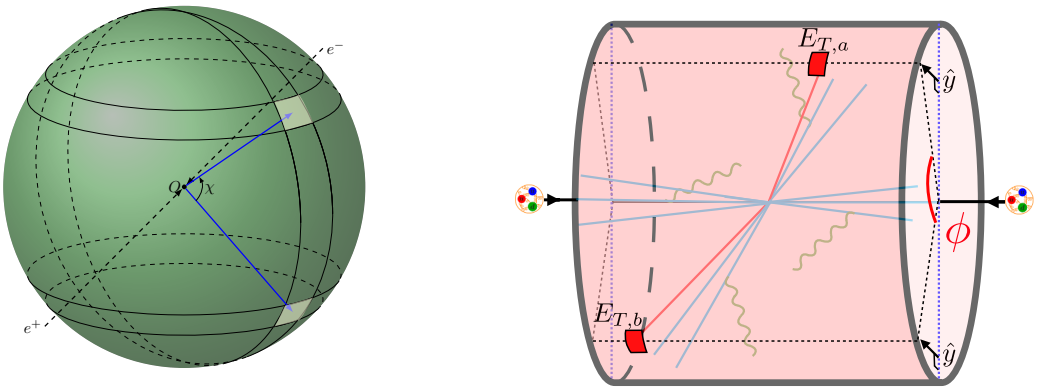

(a) (b)

Figure 1. a) The EEC observable in e^+e^- collisions measures the correlation between energy depositions as a function of the angle χ on the sphere. b) The TEEC, which generalizes the EEC to hadronic collisions, measures the correlation between energy depositions as a function of the angle ϕ in the plane transverse to the scattering.

the back-to-back (dijet) region, which is characterized by Sudakov double logarithms. The $\phi = 0$ region is characterized by a collinear limit, which exhibits single collinear logarithms. The focus in this paper will be on the back-to-back region. The resummation of the collinear logarithms can be performed similarly to the case of e^+e^- [79], which represents an extension of the jet calculus [159–161].

We can also define extensions of the TEEC for the case of $V+$ jet and Drell-Yan (or more generally arbitrary color singlet production). For the case of $V+$ jet, we define the TEEC as

$$\frac{d\sigma}{d\cos\phi} = \sum_X \int d\sigma_{pp\to V+X} \sum_{a\in X} \frac{E_{T,a}}{\sum\limits_{i\in X} E_{T,i}} \delta(\cos\phi_{Va} - \cos\phi)\,, \tag{2.3}$$

while for Drell-Yan, we define it as

$$\frac{d\sigma}{d\cos\phi} = \int d\sigma_{pp\to l^+ + l^- + X} \delta(\cos\phi_{l^+l^-} - \cos\phi)\,. \tag{2.4}$$

Note that in all cases, the definition of the TEEC is chosen such that it obeys a sum rule, namely

$$\int d\cos\phi \frac{d\sigma}{d\cos\phi} = \sigma_{\text{tot}}\,. \tag{2.5}$$

The factorization formula that we will derive will trivially also apply to these cases. We believe that having an observable defined for final states with 0, 1 and 2 final state jets, all of which can be computed at N^{3}LL, is particularly interesting from the perspective of studying factorization violation. Another interest in defining the TEEC for these additional final states, in particular $W/Z/\gamma$, is also that they might be the first to which one can match at NNLO. For recent progress towards the $pp \to V + 2$ jet amplitudes at NNLO, see [162].

We should also note that the TEEC observable is similar to other observables that measure azimuthal correlations in DIS [163] in back-to-back jets in e^+e^- or pp [147], or between jets and vector bosons [164–167].

JHEP09(2024)072

3 Factorization in the back-to-back limit

In this section, we derive the factorization formula for the TEEC in the back-to-back limit, which was first presented without derivation in [64]. Due to the simplicity of the TEEC observable, we will find that the factorization formula in this region can be expressed in terms of well known functions used in the description of other observables, but combined in a non-trivial way. This is particularly convenient, since it immediately allows us to derive all required anomalous dimensions using existing results in the literature. The factorization we present is expected to be violated at higher orders by Glauber contributions, and we discuss this in section 3.3.

3.1 Kinematics

In this subsection, we identify the relevant kinematical regions for $\phi \to \pi$. We first review the kinematics for the back-to-back limit of the EEC in e^+e^- colliders (details can be found in [77]). We then generalize this discussion to the case of a hadron collider.

In e^+e^- collisions, it is customary to define a dimensionless variable, $z = (1 - \cos\chi)/2$, where χ is the angle between two outgoing particles with momenta k_a and k_b. In the massless limit,

$$1 - z = \frac{1 + \cos\chi}{2} = \frac{k_a^0 k_b^0 + \vec{k}_a \cdot \vec{k}_b}{2k_a^0 k_b^0}\,. \tag{3.1}$$

In the back-to-back limit, k_a is almost anti-aligned with k_b, and we have

$$1 - z = \frac{1 - \cos(\pi - \chi)}{2} \sim \frac{(\pi - \chi)^2}{4} + \mathcal{O}((\pi - \chi)^4)\,. \tag{3.2}$$

At leading power, k_a and k_b must come from the splitting of two almost back-to-back jets with momentum p_1 and p_2. The two jets are not exactly back-to-back due to soft radiation. Let $\chi_J = \vec{p}_1 \cdot \vec{p}_2/(|\vec{p}_1||\vec{p}_2|)$ be the angle between the two jets. Its deviation from the exact back-to-back limit, $\chi_J = \pi$, is given by

$$\frac{(\pi - \chi_J)^2}{4} = \frac{\vec{k}_{s\perp}^2}{Q^2}\,, \tag{3.3}$$

where $\vec{k}_{s\perp}$ is the transverse momentum of the soft radiation, defined either against p_1, or p_2, or even the thrust axis of the whole event. Different choices for the axes only lead to power suppressed effects, and are thus irrelevant to the discussion in this paper. χ differs from χ_J due to transverse recoil of k_a and k_b against p_1 and p_2, respectively. Taking this into account, one obtains

$$(1 - z) \sim \left(\frac{\vec{k}_{a\perp}}{\xi_a Q} + \frac{\vec{k}_{b\perp}}{\xi_b Q} - \frac{\vec{k}_{s\perp}}{Q}\right)^2 + \mathcal{O}((1 - z)^2)\,, \tag{3.4}$$

where $\vec{k}_{a(b)\perp}$ is the transverse momentum of $k_{a(b)}$ against $p_{1(2)}$, and $\xi_{a(b)}$ is the corresponding longitudinal momentum fraction, i.e. $k_{a(b)} = \xi_{a(b)} p_{1(2)} + k_{a(b)\perp}$. The fact that $(1 - z)$ can be related to the transverse momentum of soft or collinear states leads to enormous

JHEP09(2024)072

simplifications for resummation: 1) many of the ingredients for resummation can be adopted from q_T resummation for Drell-Yan/Higgs production at hadron colliders; 2) the vector sum nature of eq. (3.4) admits a simple factorization of soft and collinear modes in impact parameter space; 3) most importantly, the soft radiation is defined globally, avoiding the need to partition the phase space into different angular directions as in the case of the beam thrust (or N-jettiness) soft function.

Now we would like to apply the above observations to the TEEC in the back-to-back limit. Much like for the EEC, it is convenient to work with the variable

$$z_\phi = \frac{1-\cos\phi}{2}\,. \tag{3.5}$$

As compared to the case of e^+e^-, we use the subscript ϕ to emphasize that this variable corresponds to the TEEC. We consider the LO partonic scattering process, $p_1 + p_2 \to p_3 + p_4$. Generalizing this to the hadronic scattering process will be straightforward in the factorization formula. At LO, the correlation localizes at $\phi \equiv 0$ in the azimuthal plane. The incoming and outgoing momentum p_i span the scattering plane, which we choose to be the x-z plane, where the z-axis is the beam axis. Non-trivial ϕ dependence is generated through radiation *out of* the scattering plane. In the back-to-back limit where $\phi \to \pi$, hard radiation out of the plane is power suppressed, enforcing that the shape of the event is almost planar. After integrating out the hard virtual contributions, the relevant low energy modes are collinear radiation in the initial and final state, as well as global soft radiation. A simple derivation shows that in this limit we have

$$1 - z_\phi = \sin^2\frac{\pi-\phi_{ab}}{2} = \frac{1}{4p_T^2}\left(\frac{k_{a,y}}{\xi_a} + \frac{k_{b,y}}{\xi_b} + p_{1,y} + p_{2,y} - k_{s,y}\right)^2 + \mathcal{O}((1-z_\phi)^2)\,. \tag{3.6}$$

Here p_1 and p_2 are initial state partons which enter the hard scattering vertex. Initial-state splittings result in non-zero transverse momentum off the scattering plane, which we denote as $p_{1,y}$ and $p_{2,y}$. k_a and k_b are the momenta of final-state particles from p_3 and p_4 respectively, whose transverse energy correlation is to be measured. They acquire non-zero transverse momentum off the scattering plane due to final-state collinear splitting. ξ_a and ξ_b are their respective longitudinal momentum fraction relative to p_3 and p_4. $k_{s,y}$ is the transverse momentum of soft radiation off the scattering plane. p_T is the LO transverse momentum of p_3 and p_4 relative to the beam axis, which plays the role of hard scale in the problem. When discussing the factorization in the back-to-back limit, we will often use

$$\tau \equiv 1 - z_\phi\,, \tag{3.7}$$

since it is the appropriate resolution variable for characterizing the back-to-back limit.

Comparing eqs. (3.4) and (3.6), one notices the close similarity between the two. The two-dimensional transverse momentum in eq. (3.4) is replaced by the one-dimension transverse momentum in eq. (3.6). There is also an additional contribution from initial-state physics in eq. (3.6). This makes clear that one should view the TEEC in the back-to-back limit as a sort of generalization of the standard q_T observable to dijet final states.

JHEP09(2024)072

3.2 Factorization formula

We can now derive a factorization formula for the TEEC in the back-to-back limit. This follows closely the derivation for the EEC in [77], which in turn builds on the factorization formula for identified hadron production in the back-to-back limit [147, 148]. In particular, we will use the approach of factorizing a multi-differential cross section in terms of beam and fragmentation functions. We will then show that the integration over this multi-differential cross section to obtain the TEEC allows the use of sum rules to eliminate non-pertubative contributions from the fragmentation functions, as expected for an Infrared and collinear safe observable. Throughout this section, we will suppress Lorentz indices for simplicity. At N^{3}LL, non-trivial spin structures give rise to interesting effects in the form of linearly polarized jet and beam functions. We will discuss these in more detail in section 6.

To derive the factorization, we start with the expression

$$\frac{d\sigma}{dz_\phi} = \frac{1}{2}\sum_{h,h'}\int d\zeta_h\, d\zeta_{h'}\, \zeta_h\, \zeta_{h'}\, \frac{d^3\sigma}{d\zeta_h d\zeta_{h'} dz_\phi}\,, \tag{3.8}$$

where h, h' are summed over all the final-state hadrons, and $\frac{d^3\sigma}{d\zeta_h d\zeta_{h'} dz_\phi}$ is the triple differential cross section measuring the transverse energy fraction with respect to the transverse energy of the jet, $\zeta_h = p_{h,T}/p_T$, and the relative angle z_ϕ. We will denote the momenta of the incoming partons as p_1^μ and p_2^μ, and p_3^μ and p_4^μ are the outgoing parton level quarks or gluons. In the limit that p_1^μ and p_2^μ have very small transverse energy, $\vec{p}_1$, $\vec{p}_2$, $\vec{p}_3$, and $\vec{p}_4$ are almost on a plane, which we denote as zx-plane, and the transverse momenta of two outgoing partons are nearly the same, which we denote p_T.

In the limit that h and h' are back-to-back, let hadrons h and h' be emitted from p_3 and p_4 respectively, so that their transverse energy fraction of $\zeta_{h(h')}$ and longitudinal momentum fraction $\xi_{h(h')}$ relative to $p_{3(4)}$ can be used interchangeably. From now on, we will replace $\zeta_{h(h')}$ in eq. (3.8) by $\xi_{h(h')}$. To leading power, we only need to consider recoil effects from soft radiation and collinear fragmentation in the y-direction, so that

$$1 - z_\phi = \sin^2\frac{\pi-\phi}{2} = \frac{1}{4p_T^2}\left|\frac{k_{h,y}}{\xi_h} + \frac{k_{h',y}}{\xi_{h'}} + p_{1,y} + p_{2,y} - k_{s,y}\right|^2 + \mathcal{O}((1-z_\phi)^2). \tag{3.9}$$

Compared with eq. (3.6), here we use h and h' instead of a and b to emphasize that they are hadrons. We can change the variable z_ϕ for the y-momentum $q_y = k_{h,y}/\xi_h + k_{h',y}/\xi_{h'} + p_{1,y} + p_{2,y} - k_{s,y}$,

$$\frac{d^3\sigma}{d\xi_h\, d\xi_{h'}\, dz_\phi} = \int dq_y\, \frac{d^3\sigma}{d\xi_h\, d\xi_{h'}\, dq_y}\,\delta\left(1 - z_\phi - \frac{q_y^2}{4p_T^2}\right). \tag{3.10}$$

We now proceed to factorize the triple differential distribution,

$$\begin{aligned}\sum_{h,h'}\frac{d^3\sigma}{d\xi_h\, d\xi_{h'}\, dz_\phi} = \frac{1}{2s}\sum_{h,h'}{\sum_X}'\langle P_1P_2|X\rangle\delta(\xi_h - k_{h,T}/p_T)\delta(\xi_h - k_{h',T}/p_T) \\ \times\,\delta\left(z_\phi - \frac{1}{2} - \frac{\vec{k}_{h\perp}\cdot\vec{k}_{h'\perp}}{2|\vec{k}_{h\perp}||\vec{k}_{h'\perp}|}\right)\langle X|P_1P_2\rangle\,,\end{aligned} \tag{3.11}$$

where s is the collision energy and we sum over all the hadronic states X. Here $|P_{1,2}\rangle$ denote the incoming proton state, and k_h and $k_{h'}$ are two detected particles. $\vec{k}_{h(h')\perp}$ is the transverse momentum of the detected particle against the beam axis. The phase space summation $\sum'_X$, is restricted by experimental cuts to select only hard scattering events. For example, the ATLAS measurement for TEEC [6, 7, 9] imposes an average $p_T \geq 250\,\text{GeV}$ for two leading jets, and rapidity $|Y| \leq 2.5$. Throughout this paper we work in the high energy limit such that the detected hadrons are taken to be massless.

In the limit of $z_\phi \to 1$, the radiation in the event is restricted to lie in a plane, as explained in section 3.1. An illustration of a typical event is depicted in figure 1(b), where there are bunches of collinear particles emitted in the beam and jet directions (shown in light blue), and soft particles emitted in all directions (shown in green). To describe the dynamics in this limit, we use the soft collinear effective theory (SCET) [100–103], which will allow us to provide a factorized description of the dynamics of the soft and collinear radiation. Since the soft and collinear modes are on the same mass shell hyperbola, SCET_{II} is used to derive the factorization formula. Throughout this section, we do not consider cross talk between the beam remnants and final-state jets, which could potentially invalidate the factorization picture (A brief discussion of factorization violation is given in section 3.3). However, there is evidence that such factorization violation effects exist due to the exchange of Glauber gluons at high orders in perturbation theory. To the accuracy considered in this paper, namely NNLO in fixed-order perturbation and N^3LL in resummed perturbation theory, we strongly believe that the factorization picture is not spoiled. At higher perturbative orders, we believe that our factorization formula can serve as a concrete foundation for a quantitative understanding of factorization violating effects at hadron collider.

To achieve a factorized description of the TEEC in the back-to-back limit, short distance physics is first integrated out and matched onto a set of SCET hard operators which describe the hard scattering. In our case, these are a set of hard operators that describe the short distance $2 \to 2$ scattering processes, e.g., $q\bar{q} \to q'\bar{q}'$, $q\bar{q} \to gg$, $gg \to gg$, etc. We will take $q\bar{q} \to q'\bar{q}'$ as the primary example in our derivation of factorization, but the generalization to other processes is straightforward. The relevant leading power SCET hard operators can be schematically written as

$$\mathcal{O}_{q\bar{q}q'\bar{q}'} = \sum_I \sum_\Gamma \mathcal{C}_I^\Gamma \bar{\chi}_2 \chi_1 \bar{\chi}'_3 \chi'_4 \Gamma t_I \,, \tag{3.12}$$

where χ_i is the gauge invariant collinear quark or anti-quark field in the lightcone direction n_i, Γ is a basis of Dirac structures, and t_I is a basis of color structures. $\mathcal{C}_I^\Gamma$ is the Wilson coefficient resulted from integrating out the hard modes. We have suppressed the color indices, Lorentz indices, and kinematical dependence in eq. (3.12).

The leading power SCET Lagrangian describing the dynamics of the TEEC can be written as

$$\mathcal{L}^{(0)} = \mathcal{L}^{(0)}_{B_1} + \mathcal{L}^{(0)}_{B_2} + \mathcal{L}^{(0)}_{J_1} + \mathcal{L}^{(0)}_{J_2} + \mathcal{L}^{(0)}_{G} \,. \tag{3.13}$$

Here $\mathcal{L}^{(0)}_G$ is the Glauber Lagrangian [53], which contributes to factorization violation. We will return to this in section 3.3, but for now we set $\mathcal{L}^{(0)}_G = 0$. Once this is done, the dynamics

JHEP09(2024)072

of the different collinear sectors exactly factorizes. This implies that the external state also factorizes into collinear and soft states,

$$|X\rangle \to |X_1\rangle|X_2\rangle|X_3\rangle|X_4\rangle|X_s\rangle\,. \tag{3.14}$$

From section 3.1 it's convenient to define an auxiliary observable

$$q_y = \frac{k_{h,y}}{\xi_h} + \frac{k_{h',y}}{\xi_{h'}} + p_{1,y} + p_{2,y} - k_{s,y} \tag{3.15}$$

where we choose the y component to be the transverse component perpendicular to the scattering plane spanned by the incoming beams and outgoing jets. Writing the triple differential distribution for $d^3\sigma/(d\xi_h\, d\xi_{h'}\, dq_y)$ in terms of SCET hard operators and fields, we obtain

$$\begin{aligned}\sum_{h,h'} \frac{d^3\sigma}{d\xi_h\, d\xi_{h'}\, dq_y} = \frac{1}{2s} \times 2 \times \sum_{X_1,X_2,X_3,X_4,X_s} \sum_{h\in X_3, h'\in X_4} &\langle P_1P_2|\mathcal{O}^\dagger_{q\bar{q}q'\bar{q}'}|X_1\rangle|X_2\rangle|X_3\rangle|X_4\rangle|X_s\rangle \\ &\times \delta(\xi_h - k_{h,T}/p_T)\delta(\xi_{h'} - k_{h',T}/p_T) \\ &\times \delta\left(q_y - \left(\frac{k_{h,y}}{\xi_h} + \frac{k_{h',y}}{\xi_{h'}} + p_{1,y} + p_{2,y} - k_{s,y}\right)\right) \\ &\times \langle X_1|\langle X_2|\langle X_3|\langle X_4|\langle X_s|\mathcal{O}_{q\bar{q}q'\bar{q}'}|P_1P_2\rangle + \text{power corrections}\,. \end{aligned} \tag{3.16}$$

At leading power, h and h' are collinear particles belonging to final-state jets X_3 and X_4, respectively. They cannot be soft, since the observable is weighted by the energy of the detected particle. An overall factor of 2 arises due to restricting h to be in jet X_3.

With the dynamics factorized, it is now a standard algebraic exercise to manipulate the operators into matrix elements separately describing the dynamics of the different collinear sectors, and the soft sector (for a detailed discussion in the context of jet cross sections at the LHC, see [168]). We can write our full expression for the leading power TEEC cross section in the back-to-back limit as

$$\begin{aligned}\frac{d\sigma^{(0)}}{dz_\phi} = \frac{1}{16\pi s^2} \sum_{\text{channels}} \sum_{IJ} \sum_{hh'} \frac{1}{(1+\delta_{f_3f_4})N_{\text{init}}} &\int \frac{dy_3 dy_4 dp_T^2}{\xi_1\,\xi_2} H_{IJ}^{f_1f_2\to f_3f_4}(p_T, y_3, y_4, \mu) \\ &\times \int d\xi_h d\xi_{h'}\, \xi_h\, \xi_{h'} \int dq_y\, \delta\left(1 - z_\phi - \frac{q_y^2}{4p_T^2}\right) \int dp_{1,y}\, dp_{2,y}\, dk_{h,y}\, dk_{h',y}\, dk_{s,y} \\ &\times \delta\left(\frac{k_{h,y}}{\xi_h} + \frac{k_{h',y}}{\xi_{h'}} + p_{1,y} + p_{2,y} - k_{s,y} - q_y\right) S_{JI}(k_{s,y}, \mu, \nu) \\ &\times B_{f_1/N_1}(p_{1,y}, \xi_1, \mu, \nu)\, B_{f_2/N_2}(p_{2,y}, \xi_2, \mu, \nu) F_{h/f_3}(k_{h,y}, \xi_h, \mu, \nu) F_{h'/f_4}(k_{h',y}, \xi_{h'}, \mu, \nu)\,, \end{aligned} \tag{3.17}$$

Here, the superscript (0) denotes that this expression describes only the leading power dynamics in the expansion about the back-to-back limit. Summing over channels includes summing over the flavors of partons f_i. N_{init} is the number of initial states averaged over in computing the cross section ($N_{\text{init}} = 2^2 \times 3^2$ for the qq initial state, $N_{\text{init}} = 2^2 \times 3 \times 8$ for the qg initial state, and $N_{\text{init}} = 2^2 \times 8^2$ for the gg initial state). S_{IJ} is the soft function, B's are beam functions, F's are fragmentation functions, and the hard function H_{IJ} is defined in terms of the Wilson coefficients $\mathcal{C}_I^\Gamma$ as

$$H_{IJ} = \sum_\Gamma \mathcal{C}_I^\Gamma \mathcal{C}_J^{\Gamma *}\,, \tag{3.18}$$

JHEP09(2024)072

with I indexing the different color structures and Γ indexing the different spins. We will describe each of these functions in more detail shortly. The variables y_3 and y_4 are the rapidities of partons p_3 and p_4, and ξ_1 and ξ_2 are the energy fractions of partons p_1 and p_2 relative to hadrons P_1 and P_2, which can be expressed as functions of the Born kinematics p_T, y_3 and y_4,

$$\xi_1 = \frac{p_T}{\sqrt{s}}\left(e^{y_3} + e^{y_4}\right), \quad \xi_2 = \frac{p_T}{\sqrt{s}}\left(e^{-y_3} + e^{-y_4}\right). \tag{3.19}$$

As currently formulated, this factorization formula is not desirable, since it is expressed in terms of transverse momentum dependent fragmentation functions (TMDFFs), which are intrinsically non-perturbative objects. However, we expect that since the TEEC is an Infrared and collinear safe observable, the only non-perturbative functions appearing in its definition should be the PDFs (or more precisely the TMDPDFs). For perturbative transverse momentum, we can perform an operator product expansion (OPE) to match the TMDFFs onto the standard fragmentation functions, allowing us to use a sum rule to eliminate the fragmentation functions from the result. We therefore briefly review the properties of the TMD fragmentation functions and their OPE, to understand how to convert them into perturbative jet functions.

The standard fragmentation functions (FFs) are defined as [153, 169–171]

$$d_{h/q}(z_h) = \frac{1}{2z_h N_c}\sum_X \int \frac{db^+}{4\pi} e^{ik_h^- b^+/(2z_h)}\,\mathrm{tr}_{\mathrm{spin}}\langle 0|\frac{\bar{n}\!\!\!/}{2}\chi_n(b^+)|h,X\rangle\langle h,X|\bar{\chi}_n(0)|0\rangle\,, \tag{3.20}$$

$$d_{h/g}(z_h) = -\frac{k_h^-}{(d-2)(N_c^2-1)z_h^2}\sum_X \int \frac{db^+}{4\pi} e^{ik_h^- b^+/(2z_h)}\,\langle 0|\mathcal{B}^\mu_{n\perp}(b^+)|h,X\rangle\langle h,X|\mathcal{B}_{n\perp\mu}(0)|0\rangle\,. \tag{3.21}$$

In eq. (3.17), the TMDFFs, denoted by F, are in the parton frame, by which we mean the frame where the parton has zero transverse momentum. However, it is easier to define the TMDFFs in the hadron frame, where hadron h has zero transverse momentum. We use D to denote the hadron-frame TMDFFs, which in position space are defined as [172]

$$D_{h/q}(\vec{b}_\perp, z_h) = \frac{1}{2z_h N_c}\sum_X \int \frac{db^+}{4\pi} e^{ik_h^- b^+/(2z_h)}\,\mathrm{tr}_{\mathrm{spin}}\langle 0|\frac{\bar{n}\!\!\!/}{2}\chi_n(b)|h,X\rangle\langle h,X|\bar{\chi}_n(0)|0\rangle\,, \tag{3.22}$$

$$D^{\mu\nu}_{h/g}(\vec{b}_\perp, z_h) = -\frac{k_h^-}{(d-2)(N_c^2-1)z_h^2}\sum_X \int \frac{db^+}{4\pi} e^{ik_h^- b^+/(2z_h)}\,\langle 0|\mathcal{B}^\mu_{n\perp}(b)|h,X\rangle\langle h,X|\mathcal{B}^\nu_{n\perp}(0)|0\rangle\,. \tag{3.23}$$

Here we have used the SCET notation, where χ_n and $\mathcal{B}^\mu_n$ are the gauge invariant n-collinear quark and gluon fields respectively. The pair of fields are separated by $b^\mu = (b^+, 0^-, \vec{b}_\perp)$, with $\vec{b}_\perp$ the conjugate variable to the parton transverse momentum relative to hadron h. $D^{\mu\nu}_{h/g}$ can be decomposed into tensor structures as

$$D^{\mu\nu}_{h/g} = \frac{g_\perp^{\mu\nu}}{d-2} D_{h/g} + \left(\frac{g_\perp^{\mu\nu}}{d-2} + \frac{b_\perp^\mu b_\perp^\nu}{b_T^2}\right) D'_{h/g}\,, \tag{3.24}$$

JHEP09(2024)072

where $b_T = |\vec{b}_\perp|$. Here, $D_{h/g}$ is the unpolarized gluon contribution, while $D'_{h/g}$ is the linearly polarized gluon contribution. We leave the discussion for the linear polarization contribution to section 6 and only consider $D_{h/g}$ in this section. A detailed discussion of the relation between the TMDFFs in the two frames can be found in [115, 116, 172]; here we simply state the result,

$$F_{h/i}(\vec{b}_\perp/z_h, z_h) = z_h^{2-2\epsilon}\, D_{h/i}(\vec{b}_\perp, z_h)\,. \tag{3.25}$$

The OPE of the TMDFF onto the standard FF, is given in momentum space by

$$F_{h/i}(\vec{k}_{h\perp}, \xi_h) = \sum_j \int \frac{dz_h}{z_h^3} d_{h/j}(z_h,\mu)\mathcal{J}_{ji}\left(\frac{\vec{k}_{h\perp}}{z_h}, \frac{\xi_h}{z_h}\right) + \text{power correction}\,, \tag{3.26}$$

where $\mathcal{J}_{ij}$ are finite matching coefficients, and $d_{h/j}$ are fragmentation functions. To convert these TMDFFs as well as their matching coefficients to the ones shown in eq. (3.17) as functions of the y-component momenta, one simply integrates out their x-components,

$$F_{h/i}(k_{h,y}, \xi_h) = \int dk_{h,x}\, F_{h/i}(\vec{k}_{h\perp}, \xi_h)\,, \qquad \text{and} \qquad \mathcal{J}_{ji}\,(k_y, \xi) = \int dk_x\, \mathcal{J}_{ji}\left(\vec{k}_\perp, \xi\right)\,, \tag{3.27}$$

so that we have

$$F_{h/i}(k_{h,y}, \xi_h) = \sum_j \int \frac{dz_h}{z_h^2} d_{h/j}(z_h)\, \mathcal{J}_{ji}\left(\frac{k_{h,y}}{z_h}, \frac{\xi_h}{z_h}\right) + \text{power correction}\,. \tag{3.28}$$

We can now simplify the factorization formula in eq. (3.17), by using sum rules to eliminate the dependence on the FF. Inserting eq. (3.28) into eq. (3.17), and changing variables to $\xi_i = \xi_h/z_h$, $\xi_j = \xi_{h'}/z_{h'}$, $k_{i,y} = k_{h,y}/z_h$, $k_{j,y} = k_{h',y}/z_{h'}$, we then find

$$\begin{aligned}
\frac{d\sigma^{(0)}}{dz_\phi} = \frac{1}{16\pi s^2} \sum_{\text{channels}} \sum_{IJ} \sum_{ij} \frac{1}{(1+\delta_{f_3 f_4})N_{\text{init}}} \int \frac{dy_3 dy_4 dp_T^2}{\xi_1\xi_2} d\xi_i d\xi_j \xi_i \xi_j \int dq_y\, \delta\left(1 - z_\phi - \frac{q_y^2}{4p_T^2}\right) \\
\times \int dp_{1,y} dp_{2,y} dk_{s,y} dk_{i,y} dk_{j,y}\, \delta\left(q_y - \left(\frac{k_{i,y}}{\xi_i} + \frac{k_{j,y}}{\xi_j} + p_{1,y} + p_{2,y} - k_{s,y}\right)\right) \\
\times H_{IJ}^{f_1 f_2 \to f_3 f_4}(p_T, y_3, y_4, \mu)\, B_{f_1/N_1}(p_{1,y}, \xi_h, \mu, \nu)\, B_{f_2/N_2}(p_{2,y}, \xi_2, \mu, \nu) S_{JI}(k_{s,y}, \mu, \nu) \\
\times \left[\sum_{hh'} \int dz_h\; z_h\; d_{h/i}(z_h,\mu) \int dz_{h'}\; z_{h'}\; d_{h'/j}(z_{h'},\mu)\right] \\
\times \mathcal{J}_{if_3}\,(\xi_i, k_{i,y}, \mu, \nu)\, \mathcal{J}_{jf_4}\,(\xi_j, k_{j,y}, \mu, \nu)\,.
\end{aligned} \tag{3.29}$$

We can now use the momentum-conservation sum rule

$$\sum_h \int dz_h\; z_h\; d_{h/j}(z_h,\mu) = 1\,, \tag{3.30}$$

to cancel the non-perturbative fragmentation functions, arriving at an expression purely in terms of the perturbative matching coefficients.

Using the Fourier representation of the delta function,

$$\begin{aligned}
&\delta\left(q_y - \left(\frac{k_{i,y}}{\xi_i} + \frac{k_{j,y}}{\xi_j} + p_{1,y} + p_{2,y} - k_{s,y}\right)\right) \\
&\qquad = \int \frac{db_y}{2\pi}\; \exp\left[-ib_y q_y + ib_y\left(\frac{k_{i,y}}{\xi_i} + \frac{k_{j,y}}{\xi_j} + p_{1,y} + p_{2,y} - k_{s,y}\right)\right]\,,
\end{aligned} \tag{3.31}$$

JHEP09(2024)072

we now go to position space, and simplify our factorized expression to

$$\begin{aligned}\frac{d\sigma^{(0)}}{dz_\phi} &= \frac{1}{16\pi s^2}\sum_{\text{channels}}\sum_{IJ}\sum_{ij}\frac{1}{(1+\delta_{f_3f_4})N_{\text{init}}}\int\frac{dy_3dy_4\,p_T dp_T^2}{\xi_1\xi_2}d\xi_i d\xi_j\,\xi_i\xi_j \\ &\times\int\frac{db_y}{2\pi}\frac{e^{-2ib_y\sqrt{1-z_\phi}\;p_T}}{\sqrt{1-z_\phi}}\,H_{IJ}^{f_1f_2\to f_3f_4}(p_T,y_3,y_4,\mu)\,S_{JI}(b_y,\mu,\nu) \\ &\times B_{f_1/N_1}(b_y,\,\xi_1,\,\mu,\,\nu)\,B_{f_2/N_2}(b_y,\,\xi_2,\,\mu,\,\nu)\,\mathcal{J}_{if_3}\left(\frac{b_y}{\xi_i},\xi_i,\mu,\nu\right)\mathcal{J}_{jf_4}\left(\frac{b_y}{\xi_j},\xi_j,\mu,\nu\right).\end{aligned} \tag{3.32}$$

Finally, we define the jet function relevant to the TEEC as

$$\begin{aligned}J_q^{\text{TEEC}}(b_y) &= \sum_i\int_0^1 d\xi\;\xi\;\mathcal{J}_{iq}\left(\frac{b_y}{\xi},\xi\right), \\ J_g^{\text{TEEC}}(b_y) &= \sum_i\int_0^1 d\xi\;\xi\;\mathcal{J}_{ig}\left(\frac{b_y}{\xi},\xi\right).\end{aligned} \tag{3.33}$$

This allows us to write the final factorized expression for the TEEC in the back-to-back limit as

$$\begin{aligned}\frac{d\sigma^{(0)}}{d\tau} &= \frac{1}{16\pi s^2\sqrt{\tau}}\sum_{\text{channels}}\frac{1}{(1+\delta_{f_3f_4})N_{\text{init}}}\int\frac{dy_3dy_4\,p_T dp_T^2}{\xi_1\xi_2}\int_{-\infty}^{\infty}\frac{db_y}{2\pi}e^{-2ib_y\sqrt{\tau}p_T} \\ &\times\text{tr}\left[\mathbf{H}^{f_1f_2\to f_3f_4}(p_T,y^*,\mu)\mathbf{S}(b_y,y^*,\mu,\nu)\right] \\ &\times B_{f_1/N_1}(b_y,\,\xi_1,\,\mu,\,\nu)\,B_{f_2/N_2}(b_y,\,\xi_2,\,\mu,\,\nu)J_{f_3}^{\text{TEEC}}(b_y,\mu,\nu)\,J_{f_4}^{\text{TEEC}}(b_y,\mu,\nu).\end{aligned} \tag{3.34}$$

Here we have used $y^* = (y_3 - y_4)/2$, to denote the single jet rapidity in the partonic center-of-mass frame. For simplicity, to make contact with the notation of [64], we have written the factorized result in terms of $\tau \equiv 1 - z_\phi$, as defined in eq. (3.7).

This provides an expression for the leading power dynamics of the TEEC in the back-to-back limit in terms of a number of remarkably simple functions combined in a highly non-trivial way, and is the primary result of this work. All the functions appearing in this formula are related in some manner to TMD dynamics. The TEEC therefore provides a natural extension of the q_T observable from color singlet production, to both $W/Z/\gamma+$ jet, and dijets.

3.2.1 Summary of factorized functions

For convenience, we now briefly summarize the known functions appearing in the TEEC factorization formula, along with their RG evolution. We postpone a discussion of the soft function, which is a new ingredient of our factorization formula, to section 4.

Hard functions. The hard functions $\mathbf{H}^{f_1f_2\to f_3f_4}$ describe the underlying microscopic scattering for the partonic channel $f_1f_2 \to f_3f_4$, and are independent of the TEEC measurement. They are obtained as the infrared finite part of the $2 \to 2$ scattering amplitudes (For a precise definition, see e.g. [173]). All relevant amplitudes are well known at one [174] and two loops [117–124]. They have recently been computed at three loops [143–146]. The NLO hard functions have been extracted in [173, 175], and the NNLO hard functions are available in a MATHEMATICA file in [176]. We use the results in [176] in our calculation.

JHEP09(2024)072

The hard functions satisfy a renormalization group equation

$$\frac{d}{d\ln\mu^2}\mathbf{H} = \frac{1}{2}\left(\mathbf{\Gamma}_H\ \mathbf{H} + \mathbf{H}\ \mathbf{\Gamma}_H^\dagger\right)\,, \tag{3.35}$$

where

$$\mathbf{\Gamma}_H = -\sum_{i<j}\mathbf{T}_i\cdot\mathbf{T}_j\gamma_{\rm cusp}\ln\frac{\sigma_{ij}\,\hat{s}_{ij}-i0}{\mu^2} + \sum_i\gamma_i\mathbf{1} + \boldsymbol{\gamma}_{\rm quad}\,, \tag{3.36}$$

where $\sigma_{ij}=-1$ if both i and j are incoming or outgoing, and 1 otherwise. $s_{ij}=2p_i\cdot p_j$ are the Mandelstam variables. Here $\gamma_i=\gamma_q$, γ_g are the quark or gluon anomalous dimension. This equation describes a non-trivial matrix evolution in the color space, and its solution will be discussed in detail in section 5. The color space notation of [177] has been used here.

Beam function. The beam functions appearing in the factorization formula for the TEEC can be obtained from the standard TMD beam functions. Unlike for the transverse momentum spectrum of color singlet particles, the TEEC only measures the component of the momentum out of the plane (recall that we have taken the Born scattering process to lie in the xz-plane, so the momentum component out of the plane is the y-component). To obtain the TEEC beam function from the standard TMD beam functions, we must therefore project them onto the y-component. We first review the TMD beam functions, and then discuss their projection for the TEEC.

The TMD beam functions are defined in terms of gauge invariant SCET fields as [178]

$$\begin{aligned}
B_q(z=\omega/P_n^-,\vec{b}_\perp) &= \langle P(P_n)|\bar{\chi}_n(b_\perp)\frac{\bar{n}\!\!\!/}{2}[\delta(\omega-\bar{\mathcal{P}}_n)\chi_n(0)]|P(P_n)\rangle\,,\\
B_g^{\mu\nu}(z=\omega/P_n^-,\vec{b}_\perp) &= -\omega\,\langle P(P_n)|\mathcal{B}_{n\perp}^\mu(b_\perp)[\delta(\omega-\bar{\mathcal{P}}_n)\mathcal{B}_{n\perp}^\nu(0)]|P(P_n)\rangle\,.
\end{aligned} \tag{3.37}$$

Lorentz invariance allows the gluon TMD beam functions to be decomposed as

$$B_g^{\mu\nu}\left(z,\vec{b}_\perp\right) = \frac{g_\perp^{\mu\nu}}{2}B_g\left(z,\vec{b}_\perp\right) + \left(\frac{b_\perp^\mu b_\perp^\nu}{b_\perp^2}-\frac{g_\perp^{\mu\nu}}{2}\right)B_g'\left(z,\vec{b}_\perp\right), \tag{3.38}$$

where the second term is referred to as the linearly polarized contribution. Physically, these linearly polarized terms correspond to contributions that have an azimuthal dependence on the angle out of the hard scattering plane. We will discuss in detail the linearly polarized contributions to the beam and jet functions in section 6.

The TMD beam functions obey the μ and ν evolution equations

$$\begin{aligned}
\mu\frac{\mathrm{d}}{\mathrm{d}\mu}B_i(z,\vec{b}_\perp,\mu,\nu) &= \gamma_B(\mu,\omega,\nu)B_i(z,\vec{b}_\perp,\mu,\nu)\,,\\
\nu\frac{\mathrm{d}}{\mathrm{d}\nu}B_i(z,\vec{b}_\perp,\mu,\nu) &= \gamma_\nu^B(\vec{b}_\perp,\mu)B_i(z,\vec{b}_\perp,\mu,\nu)\,,
\end{aligned} \tag{3.39}$$

where $i=q,g$. The anomalous dimensions are given by

$$\begin{aligned}
\gamma_B(\mu,\omega,\nu) &= 2\Gamma_{\rm cusp}[\alpha_s(\mu)]\ln\frac{\nu}{\omega}-2\gamma_C^i-\frac{\gamma_S}{2}\,,\\
\gamma_\nu^B(\vec{b}_\perp,\mu) &= -\frac{1}{2}\gamma_\nu(\vec{b}_\perp,\mu)\,.
\end{aligned} \tag{3.40}$$

Here $\omega = zE_{\rm cm}$ is the large lightcone momentum.

JHEP09(2024)072

The beam functions for the TEEC can now be straightforwardly obtained from the TMD beam functions with the replacement

$$b_\perp^\mu \to b_y y^\mu \,, \tag{3.41}$$

where y^μ is a unit vector in the y-direction, which is orthogonal to the plane of the Born scattering process. This projection is trivial for the standard beam function, but gives rise to an interesting azimuthal dependence for the linearly polarized beam function

$$B_g^{\mu\nu}\left(z, b_y y^\mu\right) = \frac{g_\perp^{\mu\nu}}{2} B_g\left(z, b_y y^\mu\right) + \left(y^\mu y^\nu - \frac{g_\perp^{\mu\nu}}{2}\right) B_g'\left(z, b_y y^\mu\right) . \tag{3.42}$$

However, conveniently, the TEEC beam function can be obtained directly from the TMD beam function, allowing us to use the high loop results available in the literature

The beam functions for the TEEC can be matched onto standard PDFs at small but perturbative transverse momentum,

$$B_{i/N}(b_y, \xi, \mu, \nu) = \sum_j \int \frac{dz}{z} \mathcal{I}_{ij}\left(z, L_b, L_Q\right) f_{j/N}\left(\frac{\xi}{z}, \mu\right) + \text{power corrections}\,, \tag{3.43}$$

where $L_b = \ln(b_y^2\mu^2/b_0^2)$, $b_0 = 2e^{-\gamma_E}$, and $L_Q = \ln(Q^2/\nu^2)$, with $Q = 2p_i^0$, twice the energy of the measured parton energy. The matching coefficients have been derived to two loops in [111–116], and three loops in [138–141].

Jet functions. The jet functions appearing in the TEEC were already discussed in some detail in the derivation of the factorization formula, since it was necessary to perform an OPE of the TMDFFs onto standard FFs to obtain a factorization formula expressed entirely in terms of perturbative functions.

Definitions for the jet functions appearing in the factorization theorem for the EEC in e^+e^- collisions were first presented in [77], where it was shown that they could be obtained as moments of the TMD matching coefficients $\mathcal{J}_{ij}$. The relation between the TEEC jet functions and the EEC jet functions is identical to the relation between the TEEC beam functions and the TMD beam functions, namely one must project them onto the component perpendicular to the hard scattering plane using the substitution $b_\perp^\mu \to b_y y^\mu$. This is convenient, since the EEC jet functions are known at two- [115, 116] and three- [139, 140] loops, allowing us to immediately obtain the TEEC jet functions at the same order.

Explicitly, the jet functions appearing in the TEEC factorization formula can be obtained from the EEC jet functions by the substitution,

$$\begin{aligned} J_q^{\text{TEEC}}(b_y) &= J_q^{\text{EEC}}(b_T = b_y) = \sum_i \int_0^1 d\xi\, \xi\, \mathcal{J}_{iq}\left(\frac{b_y}{\xi}, \xi\right) , \\ J_g^{\text{TEEC}}(b_y) &= J_g^{\text{EEC}}(b_T = b_y) = \sum_i \int_0^1 d\xi\, \xi\, \mathcal{J}_{ig}\left(\frac{b_y}{\xi}, \xi\right) , \end{aligned} \tag{3.44}$$

and are obtained as moments of the (matching coefficients of the) TMD fragmentation functions. Here we have suppressed Lorentz indices. Just as for the beam function, one

JHEP09(2024)072

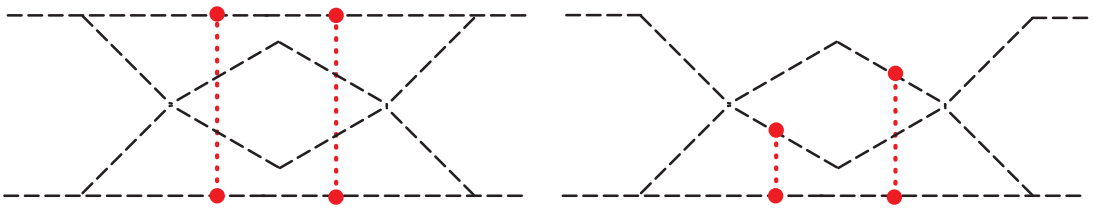

(a) (b)

Figure 2. Examples of Glauber diagrams which could violate our factorization formula for the TEEC. The Glaubers, which are illustrated by dashed red lines, couple distinct collinear sectors. For the TEEC, pure spectator graphs, such as shown in a) cancel, while graphs that involve both active and spectator partons, such as shown in b), are not expected to cancel.

also has linearly polarized jet functions. We will discuss their structure in section 6. The RG evolution of the jet functions was derived in [77] from the known evolution of the TMD fragmentation functions. It is given by

$$\mu \frac{dJ_q^{\rm TEEC}(b_y,\mu,\nu)}{d\mu} = \left[-\Gamma_{\rm cusp}(\alpha_s)\ln\frac{Q^2}{\nu^2} + 2\gamma^J_{\rm EEC}(\alpha_s)\right] J_q^{\rm TEEC}(b_y,\mu,\nu)\,, \tag{3.45}$$

for the μ evolution, and

$$\nu \frac{dJ_q^{\rm TEEC}(b_y,\mu,\nu)}{d\nu} = \left[\int_{b_0^2/b_y^2}^{\mu^2} \frac{d\bar{\mu}^2}{\bar{\mu}^2}\Gamma_{\rm cusp}(\alpha_s(\bar{\mu})) - \gamma^r_{\rm EEC}(\alpha_s(b_0/b_y))\right] J_q^{\rm TEEC}(b_y,\mu,\nu)\,, \tag{3.46}$$

for the ν evolution.

3.3 Underlying event and factorization violation

Before continuing, we must make several comments regarding the validity of our factorization formula. As described earlier, the leading power SCET Lagrangian describing the TEEC in the back-to-back limit can be written as

$$\mathcal{L}^{(0)} = \mathcal{L}^{(0)}_{B_1} + \mathcal{L}^{(0)}_{B_2} + \mathcal{L}^{(0)}_{J_1} + \mathcal{L}^{(0)}_{J_2} + \mathcal{L}^{(0)}_{G}\,, \tag{3.47}$$

where the Glauber Lagrangian [53], $\mathcal{L}^{(0)}_G$, which was set to zero in our derivation, couples the different collinear directions, leading to potential violations of our formula. Example diagrams involving Glaubers are shown in figure 2, where the Glauber gluons are shown as red-dashed lines. In the above derivation, we have assumed that the Glauber Lagrangian does not contribute, which allows us to derive a factorized formula expressed in terms of functions describing the soft and collinear sectors with no connection other than through kinematics. Full proofs of factorization have been given for Drell-Yan production, and the q_T spectrum in Drell-Yan production, in the seminal works of [147–153]. For the case of the TEEC considered here, it is expected that Glaubers will contribute and factorization will be violated. The TEEC is closely related to momentum imbalance dijet event shapes, for which there is a growing body of evidence that factorization is violated [37–53]. This ultimately arises due to amplitude-level factorization violation [44, 45, 50].

JHEP09(2024)072

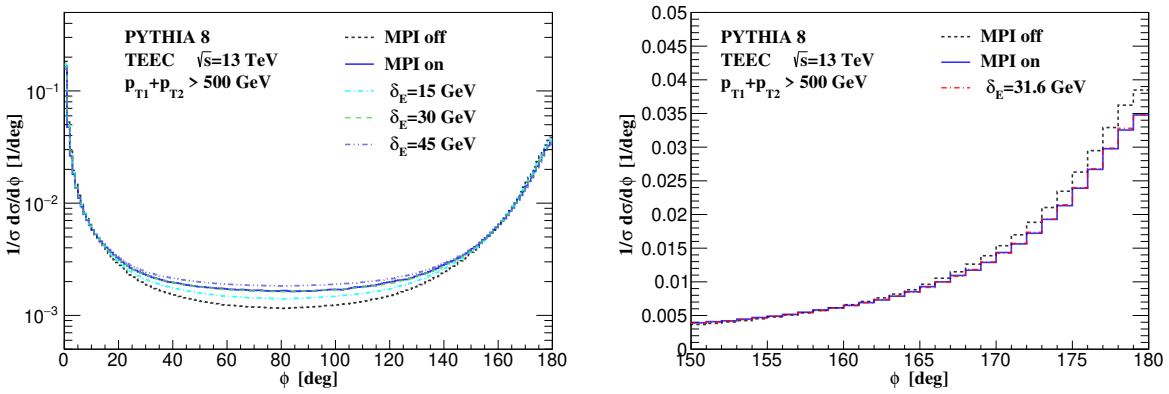

(a) (b)

Figure 3. The sensitivity of the TEEC to underlying event as modeled in Pythia. In a) we show the full distribution, while in b) we show a zoomed in version of the back-to-back endpoint region. The effects of the underlying event are small, and consistent with being a power correction. We also show the result of using a model for the underlying event, which adds a uniform energy contribution, as described in the text. We see that this simple model provides an excellent description of the effects of the underlying event throughout the entire distribution.

There are a number of different effects that can break factorization. First, even in the case of color singlet production, the imposition of a measurement function can block the cancellation of Glauber gluons arising from spectator interactions such as shown in figure 2(a). This can lead to a violation of factorization [42, 43, 53], as happens for E_T, or beam thrust. This type of factorization violation can lead to large corrections to observables, often characterized by their sensitivity to multi-parton interactions (MPI). This has been studied using a parton shower model for MPI in [179], and analytic models in [180]. Additionally, when there are jets in the initial and final states, one can have an intrinsic failure of collinear factorization [44, 50]. For the case of the TEEC, in principle both types of factorization violation could contribute to the observable.

When discussing factorization violation, one must distinguish two types of factorization violation, namely perturbative, i.e. at a scale $\gg \Lambda_{\rm QCD}$, and non-perturbative, namely at a scale $\sim \Lambda_{\rm QCD}$. Non-perturbative factorization violation would imply that one could not factorize into universal PDFs. For color singlet production, this would mean that the two beams are non-perturbatively coupled, while with jets in the final state, it would imply some non-perturbative coupling of the jets and the beams. Perturbative factorization violation, on the other hand, can be explicitly calculated in perturbation theory, and therefore is less of a concern unless it leads to infrared divergence in the cross section.

When the TEEC scale is perturbative, from the perspective of modes at the scale $\Lambda_{\rm QCD}$, the TEEC measurement is inclusive over the final state, and we expect a cancellation of the non-perturbative Glaubers. In this case, factorization violation is expected to be a power correction. However, this argument can be violated if there are many successive spectator interactions leading to a numerically large correction. This is particularly dangerous for observables that are scalar sums. On the other hand, since the TEEC is related to a vector sum, we expect it to be well behaved. In particular, we expect it to be a numerically true statement

JHEP09(2024)072

that non-perturbative factorization violation is a power correction. This can be tested at a qualitative level in parton shower Monte Carlo using a model for the underlying event.

In figure 3, we illustrate the sensitivity of the TEEC to underlying event, as modelled in Pythia [181, 182]. In figure 3(a) we show a plot over the whole range of the TEEC, while in figure 3(b), we have zoomed into the back-to-back region. We see that overall the effects of the underlying event are quite small, except right in the endpoint region where the scale probed by the TEEC reaches $\Lambda_{\rm QCD}$. We believe that this minimal sensitivity to the underlying event is quite promising, and ensures that the high perturbative accuracy of our calculation is not destroyed by underlying event. We note that this is a significantly different behavior than for the case of beam thrust, where large contributions from the underlying event are observed (see e.g. [179]).

Interestingly, we can provide an excellent description of the underlying event by adding an energy distribution that is uniform in the azimuthal angle to our perturbative calculation. Inserting a shift in the energies into the formula for the TEEC in eq. (2.2), and expanding, we find that this shifts the TEEC distribution as

$$\frac{1}{\sigma_{\rm MPI}}\frac{d\sigma_{\rm MPI}}{d\phi} = \frac{Q}{Q+2\delta_E}\left(\frac{1}{\sigma}\frac{d\sigma}{d\phi} + \frac{2}{\pi}\frac{\delta_E}{Q}\right), \tag{3.48}$$

where δ_E is the total energy added by MPI effects and $Q = 500\,\text{GeV}$ is an approximation to the total transverse energy of the hard scattering that will be used in our numerical results. The result of this model is also shown in figure 3. We see that it provides an excellent description of Pythia's model of the underlying event for a value of the parameter $\delta_E \sim 30\,\text{GeV}$. It would be interesting to measure this in experiment, and also to study its variation with the hard scattering energy. The apparent simplicity of this description of the underlying event may also allow it to be distinguished from hadronization effects. This has been studied for the jet mass in [183], and it would be interesting to perform a similar study for the TEEC.

We can also ask to what extent our factorization formula can be violated perturbatively. For E_T and beam thrust, perturbative factorization violation occurs at N^4LL [42, 43, 53], through diagrams such as the one shown in figure 2(a). While a complete analysis of perturbative Glauber contributions is beyond the scope of this paper, we make several additional comments. First, we note that due to the measurement restriction being a vector sum, following the arguments in [53], diagrams with Glaubers exchanged purely between spectators, such as in figure 2(a), are expected to cancel for the TEEC. However, we do believe that factorization will be violated by diagrams such as those shown in figure 2(b), which we believe could give at most a constant at three loops. As has been shown, it is expected that factorization violation should occur when there are two Glaubers, one collinear emission, and one additional emission [44, 50]. We strongly expect that this is an N^4LL effect. For the case of so called super-leading logarithms [46–51], these effects modify the structure of the logarithmic series. However, this arises since there are only single logarithms in the observables of interest in their work. In our case we do not expect this to be the case, however, we have not yet proven this assertion.

Nevertheless, we believe that pushing to as high perturbative orders as possible is useful, since our factorization formula can be viewed as a baseline, on which factorization violating effects can be added. We believe that due to the simplicity of the TEEC, it is an ideal

JHEP09(2024)072

observable to attempt to analytically understand the violation of factorization with final state jets using the Glauber Lagrangian of [53]. We believe that this is particularly true due to the fact that, as discussed in section 2, the TEEC can be defined for a color singlet final state, for a final state with a single jet, and for dijets final state. Since it is known that for the case of a color singlet factorization holds to all orders for the TEEC (since it is related to the factorization for transverse momentum of a color singlet boson), and that it is certainly violated for a dijet final state, we believe that this provides an extremely concrete playground to understand theoretically, and also probe experimentally, the effects of factorization violation. We leave this to future work.

3.4 Extension to Drell-Yan and $W/Z/\gamma$ + jet

Although the focus in this paper is on the TEEC for a purely hadronic final state (which at leading power in the back-to-back limit is a dijet final state), as we have discussed previously, we find it interesting that we can also achieve the same level of perturbative accuracy for the TEEC as measured on a leptonic final state in Drell-Yan, or on a $W/Z/\gamma+$ jet final state, and we believe that this will be useful for studying the effects of factorization violation. Therefore, for completeness, we also present the factorization formulas for the TEEC as measured on these final states. All of the relevant factorization formulas can be trivially obtained starting from the factorization formula for the purely hadronic final state, by removing jet functions, altering the Wilson line structure in the soft functions, and using the appropriate hard functions (For recent progress in the calculations of the relevant hard functions, see [184, 185]).

For the case of Drell-Yan, we can simply eliminate the two jet functions, and obtain

$$\begin{aligned}\frac{d\sigma^{(0)}}{d\tau} = \frac{1}{16\pi s^2\sqrt{\tau}} \sum_{\text{channels}} \frac{1}{N_{\text{init}}} \int \frac{dy_{l^+}\, dy_{l^-}\, p_T dp_T^2}{\xi_1\xi_2} \int_{-\infty}^{\infty} \frac{db_y}{2\pi} e^{-2ib_y\sqrt{\tau}p_T} \\ \times \text{tr}\big[\mathbf{H}^{f_1f_2\to l^+l^-}(p_T, y^*, \mu)\mathbf{S}(b_y, y^*, \mu, \nu)\big] B_{f_1/N_1}(b_y,\, \xi_1,\, \mu,\, \nu)\, B_{f_2/N_2}(b_y,\, \xi_2,\, \mu,\, \nu)\,.\end{aligned} \tag{3.49}$$

This is similar to the factorization for the transverse momentum of the vector boson. For the case of $V+$ jet, we have

$$\begin{aligned}\frac{d\sigma^{(0)}}{d\tau} = \frac{1}{16\pi s^2\sqrt{\tau}} \sum_{\text{channels}} \frac{1}{N_{\text{init}}} \int \frac{dy_3 dy_V\, p_T dp_T^2}{\xi_1\xi_2} \int_{-\infty}^{\infty} \frac{db_y}{2\pi} e^{-2ib_y\sqrt{\tau}p_T} \\ \times \text{tr}\big[\mathbf{H}^{f_1f_2\to f_3V}(p_T, y^*, \mu)\mathbf{S}(b_y, y^*, \mu, \nu)\big] B_{f_1/N_1}(b_y,\, \xi_1,\, \mu,\, \nu) \\ \times B_{f_2/N_2}(b_y,\, \xi_2,\, \mu,\, \nu) J_{f_3}\,(b_y, \mu, \nu)\,.\end{aligned} \tag{3.50}$$

Renormalization group consistency holds for all these different factorization formulas. We have used the same notation for the soft functions appearing in all the TEEC factorization formulas, despite the fact that they contain different numbers of Wilson lines. The precise definitions of the soft functions, as well as a discussion of their perturbative structure will be given in section 4.

It would be extremely interesting to study the effects of underlying event and factorization violation for these the TEEC observable on different final states, particularly since factorization has been proven to hold for the TEEC on color singlet final states [147–153]. This provides a baseline on top of which factorization violation and color flow effects can be studied. We leave detailed phenomenological studies of the different final states to future work.

JHEP09(2024)072

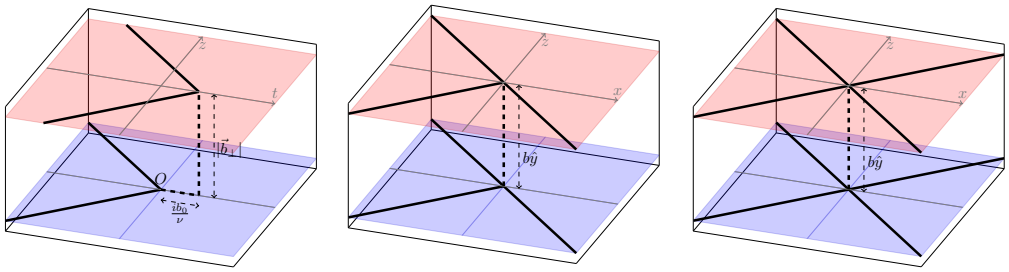

(a) (b) (c)

Figure 4. The TEEC soft functions defined using the exponential rapidity regulator for (a) TEEC for Drell-Yan (or q_T), (b) TEEC for $W/Z/\gamma+$ jet, (c) TEEC for dijets.

4 The transverse energy-energy correlator soft function

The key new perturbative ingredient entering our factorization formula is the TEEC soft function. For multi-jet event shape observables, the soft function is typically the most complicated function entering the factorization formula, since it depends on the directions of all the different jets (For recent progress towards numerical calculations of soft functions at NNLO, see [186–189], and for a semi-numerical calculation of the soft function for 2-jettiness, see [190].). In this section, we highlight the remarkable perturbative simplicity of the TEEC soft function, and we describe how this is related to the particular form of the measurement.

The structure of the TEEC soft function is also of intrinsic theoretical interest, since it provides an example of a rapidity divergent soft function with multiple (> 2) Wilson line directions. While the structure of rapidity divergences and their associated renormalization group evolution for soft functions involving two directions is by now quite well understood (the rapidity anomalous dimension is known to four loops in both QCD [16, 106, 142] and $\mathcal{N} = 4$ super Yang-Mills [191]), and has been used to make phenomenological predictions at N^{3}LL [192], almost nothing is known about the rapidity anomalous dimension for soft functions involving multiple directions. Part of the understanding of the structure of rapidity divergences comes from the fact that for the particular case of two directions, they are related by conformal symmetry to standard anomalous dimensions [142, 193, 194]. It would therefore be interesting to understand to what extent this holds more generally, and the TEEC provides a concrete example where these questions can be studied.

In section 4.1 we define the TEEC soft function and give its renormalization group evolution. In sections 4.2 and 4.3 we present some details of the calculation of the soft function at one and two loops. We then summarize our findings and discuss some directions for future study in section 4.4.

JHEP09(2024)072

4.1 Definition and RG evolution

In this section, we will discuss simultaneously the TEEC soft functions for Drell-Yan, $W/Z/\gamma+$ jet and dijets. The TEEC soft functions are defined, using the exponential regulator of [195], as

$$\begin{aligned}
\text{Drell-Yan}: &\quad \mathbf{S}(b_y, y^*) = \langle 0|T[\boldsymbol{O}_{n_1 n_2}(0^\mu)]\overline{T}[\boldsymbol{O}^\dagger_{n_1 n_2}(b_y^\mu)]|0\rangle\,, \\
W/Z/\gamma\text{+jet}: &\quad \mathbf{S}(b_y, y^*) = \langle 0|T[\boldsymbol{O}_{n_1 n_2 n_3}(0^\mu)]\overline{T}[\boldsymbol{O}^\dagger_{n_1 n_2 n_3}(b_y^\mu)]|0\rangle\,, \\
\text{Dijets}: &\quad \mathbf{S}(b_y, y^*) = \langle 0|T[\boldsymbol{O}_{n_1 n_2 n_3 n_4}(0^\mu)]\overline{T}[\boldsymbol{O}^\dagger_{n_1 n_2 n_3 n_4}(b_y^\mu)]|0\rangle\,,
\end{aligned} \tag{4.1}$$

as illustrated in figure 4 (There the temporal direction has necessarily been suppressed in (b) and (c)). Here $\boldsymbol{O}_{n_1 n_2}(x) = \boldsymbol{Y}_{n_1}\boldsymbol{Y}_{n_2}(x)$, $\boldsymbol{O}_{n_1 n_2 n_3}(x) = \boldsymbol{Y}_{n_1}\boldsymbol{Y}_{n_2}\boldsymbol{Y}_{n_3}(x)$, and $\boldsymbol{O}_{n_1 n_2 n_3 n_4}(x) = \boldsymbol{Y}_{n_1}\boldsymbol{Y}_{n_2}\boldsymbol{Y}_{n_3}\boldsymbol{Y}_{n_4}(x)$, with $\boldsymbol{Y}_{n_i}(x) = \exp[i\int ds\, n_i \cdot A_s(sn_i + x)\mathbf{T}_i]$ a semi-infinite light-like soft Wilson line, and $n_i^\mu = p_i^\mu/p_i^0$ the light-like direction of the incoming or outgoing parton in the partonic center-of-mass frame. The directions of the Wilson lines are standard and hence suppressed, as are gauge links at infinity. We have chosen coordinates such that $b_y^\mu = (0^+, 0^-, 0_x, b_y)$ is in the direction $\hat{y}$ perpendicular to the scattering plane, $\hat{y}\cdot n_i = 0$.

The soft functions defined in eq. (4.1) suffer from UV and rapidity divergences. Rapidity divergences are regulated using the exponential regulator of [195]. The soft function, which is a matrix in color space, satisfies the RG equation

$$\frac{d\mathbf{S}}{d\ln\mu^2} = \frac{1}{2}\left(\boldsymbol{\Gamma}_S^\dagger \cdot \mathbf{S} + \mathbf{S}\cdot\boldsymbol{\Gamma}_S\right)\,, \tag{4.2}$$

with [196–199]

$$\boldsymbol{\Gamma}_S = \sum_{i<j}\mathbf{T}_i\cdot\mathbf{T}_j\gamma_{\text{cusp}}\ln\frac{\sigma_{ij}\nu^2\, n_i\cdot n_j - i0}{2\mu^2} - \sum_i\frac{c_i}{2}\gamma_s\mathbf{1} - \boldsymbol{\gamma}_{\text{quad}}\,, \tag{4.3}$$

where $\sigma_{ij} = -1$ if both i and j are incoming or outgoing, and $\sigma_{ij} = 1$ otherwise. Here ν is the rapidity scale, and $c_i = C_F$ or C_A is the Casimir of the parton i. Here γ_{cusp} is the cusp anomalous dimension [200], γ_s is the threshold soft anomalous dimension [201] and $\boldsymbol{\gamma}_{\text{quad}}$ is the anomalous dimension for quadrupole color and kinematic entanglement, which first appears at three loops [104, 105] for the case that there are four Wilson lines. Its structure will be discussed in section 5, where we will also discuss the solution of the RG evolution equation with color mixing.

The evolution equation associated with the rapidity scale ν is

$$\frac{d\mathbf{S}}{d\ln\nu^2} = \frac{1}{2}\left(\boldsymbol{\Gamma}_y^\dagger\cdot\mathbf{S} + \mathbf{S}\cdot\boldsymbol{\Gamma}_y\right)\,, \tag{4.4}$$

with

$$\boldsymbol{\Gamma}_y = \left(\int_{\mu^2}^{b_0^2/b_y^2}\frac{d\bar{\mu}^2}{\bar{\mu}^2}\gamma_{\text{cusp}}[\alpha_s(\bar{\mu})] + \gamma_r[\alpha_s(b_0/b_y)]\right)\sum_i c_i\mathbf{1} + \boldsymbol{\gamma}_X[y^*, \alpha_s(b_0/b_y)]\,. \tag{4.5}$$

This is the generalization of the rapidity RGE [202, 203] for color singlet production to dijet production at hadron colliders. Here γ_r is the rapidity anomalous dimension for the color transverse momentum distribution [106], and $b_0 = 2e^{-\gamma_E}$.

JHEP09(2024)072

Thanks to the non-abelian exponentiation theorem [204, 205], we can write the TEEC soft function as an exponential of web diagrams. We further separate web diagrams into dipole, tripole and quadrupole contributions, by which we mean interactions involving two, three, and four Wilson lines respectively,

$$\mathbf{S} = \exp\Big[\mathbf{S}_{\rm dip} + \mathbf{S}_{\rm tri} + \mathbf{S}_{\rm quad}\Big] \,. \tag{4.6}$$

The dipole contribution starts at $\mathcal{O}(\alpha_s)$, where the calculation is naturally expressed as a sum over dipoles. We will show in section 4.2 that[1]

$$\mathbf{S}_{\rm dip} = -\sum_{i<j} \mathbf{T}_i \cdot \mathbf{T}_j \, S_{ij} = -\sum_{i<j} \mathbf{T}_i \cdot \mathbf{T}_j \, S_\perp \left(L_b, L_\nu + \ln \frac{n_i \cdot n_j}{2}\right) , \tag{4.7}$$

where $S_\perp(L_b, L_\nu)$ is the TMD soft function for color singlet production at hadron colliders (which can be found up to three loops in [106])

The tripole soft function starts at $\mathcal{O}(\alpha_s^2)$; we will calculate it in section 4.3. The quadrupole contribution starts at three loop: its μ dependent part is predicted by $\boldsymbol{\gamma}_{\rm quad}$, while the constant piece is beyond the scope of this paper.

We note that if there were no $\mathbf{S}_{\rm tri}$ and $\mathbf{S}_{\rm quad}$, the dipole contribution alone already satisfies the rapidity RGE (4.4). Rapidity RG consistency then implies that $\mathbf{S}_{\rm tri}$ and $\mathbf{S}_{\rm quad}$ are both free from rapidity divergences. We call the statement that rapidity divergences in the soft function take a dipole form (or equivalently, that $\mathbf{S}_{\rm tri}$ and $\mathbf{S}_{\rm quad}$ are both free from rapidity divergences) the "rapidity dipole conjecture". We will show in section 4.3 that for $\mathbf{S}_{\rm tri}$ this is indeed the case to two loops. However, it is far from obvious that $\mathbf{S}_{\rm tri}$ and $\mathbf{S}_{\rm quad}$ will be free from rapidity divergences at higher loop order. It would be particularly interesting to prove or to disprove the dipole conjecture. If the dipole conjecture turns out to be wrong, it implies factorization violation.

While the renormalization group evolution predicts the logarithmic structure of the soft functions, to achieve N^{3}LL accuracy, we also need the soft function constants to two loops (which provide the boundary conditions for the RG evolution).

4.2 Dipole contribution

In this section, we will show that each dipole soft function with general n_i and n_j can be written as $S_\perp$ with ν^2 modified by the $n_i \cdot n_j/2$ factor

We will perform a one loop calculation to demonstrate this. In the exponential rapidity regulator of [195], the bare one loop integral for each dipole soft function is given by

$$S_{ij}(b_y, \tau) = 2(4\pi)^2 \left(\frac{\mu^2 e^{\gamma_E}}{4\pi}\right)^{\frac{4-d}{2}} \int \frac{d^d k \, \delta^+(k^2)}{(2\pi)^{d-1}} \frac{n_i \cdot n_j}{(k\cdot n_i)(k\cdot n_j)} \exp\left(-2k_0 \tau e^{-\gamma_E} + \mathrm{i} b_y \cdot k\right) , \tag{4.8}$$

where $d = 4 - 2\epsilon$, $\delta^+(k^2) = \theta(k_0)\delta(k^2)$, and b_y is the impact parameter perpendicular to the scattering plane, $b_y^\mu = (0^+, 0^-, 0_x, b_y)$. τ here is the rapidity regulator: at the end of the

[1] We have assumed here that the TMD soft function S_{ij} takes the same expression no matter i and j being incoming or outgoing. In [206], it was argued with contour deformation that the TMD soft function takes the same universal expression for Drell-Yan, e^+e^- and semi-inclusive deep elastic scattering. It would be interesting to use the Glauber SCET [53] to prove or disprove this.

JHEP09(2024)072

calculation, one keeps the leading term of $\tau \to 0$ and identify $\nu = \tau^{-1}$. We work in the $\overline{\text{MS}}$ scheme by a redefinition of the bare scale $\mu_0^2 = \mu^2 e^{\gamma_E}/(4\pi)$. We then rescale $n_{i,j}$ to $\tilde{n}_{i,j}$ as

$$\tilde{n}_i = \frac{n_i}{\sqrt{(n_i \cdot n_j)/2}}\,, \qquad \tilde{n}_j = \frac{n_j}{\sqrt{(n_i \cdot n_j)/2}}\,, \tag{4.9}$$

such that $\tilde{n}_i \cdot \tilde{n}_j = 2$, and work in the lightcone frame in terms of $\tilde{n}_i$ and $\tilde{n}_j$, i.e., we decompose momentum k as,

$$k^\mu = \frac{k^+}{2}\tilde{n}_j^\mu + \frac{k^-}{2}\tilde{n}_i^\mu + k_\perp^\mu\,, \tag{4.10}$$

where $k^+ = \tilde{n}_i \cdot k$, $k^- = \tilde{n}_j \cdot k$. The one loop bare soft function now becomes

$$\begin{aligned} S_{ij}(b_y, \tau) = 2(4\pi)^2 \left(\frac{\mu^2 e^{\gamma_E}}{4\pi}\right)^{2-d/2} \int \frac{dk^- dk^+ d^{d-2}k_\perp}{2(2\pi)^{d-1}} \delta^+(k^2) \frac{2}{k^+ k^-} \\ \times \exp\left(-\left[\sqrt{\frac{n_i \cdot n_j}{2}}\,(k^+ + k^-) + v_\perp \cdot k\right] \tau e^{-\gamma_E} + \mathrm{i} b_y \cdot k\right)\,. \end{aligned} \tag{4.11}$$

Comparing this integral with the one-loop calculation in [195], we see that the only difference is that $2k_0$ is replaced by the term in the square bracket instead of simply $k^+ + k^-$. Here $v_\perp$ is a perpendicular vector. The $v_\perp \cdot k$ part does not matter when we take the $\tau \to 0$ limit since its contribution is $\mathcal{O}(\tau)$ suppressed compared with $\mathrm{i} b_y \cdot k$. The $\sqrt{\frac{n_i \cdot n_j}{2}}$ is a multiplicative factor to τ, which amounts to dividing ν^2 by $\frac{n_i \cdot n_j}{2}$ in the final result.

We expect that a similar argument can be generalized to all loop orders since there is only single logarithm for ν (or single pole in η for the η regulator [202, 203]) in the exponential of the soft function, and thus the subleading terms in $\tau \to 0$ do not matter.

Note that for $2 \to 2$ kinematics, we have the following kinematic relations

$$\begin{aligned} n_1 \cdot n_2 &= n_3 \cdot n_4 = 2\,, \\ n_1 \cdot n_3 &= n_2 \cdot n_4 = -\frac{2\hat{t}}{\hat{s}}\,, \\ n_1 \cdot n_4 &= n_2 \cdot n_3 = -\frac{2\hat{u}}{\hat{s}}\,, \end{aligned} \tag{4.12}$$

where $\hat{s} = (p_1 + p_2)^2$, $\hat{t} = (p_1 - p_3)^2$ and $\hat{u} = (p_2 - p_3)^2$ are the partonic Mandelstam variables.

4.3 Tripole contribution at two loops

In this section, we calculate the "tripole" contribution that arises at two loops, which correlates three lines in the soft function. We will show that it is purely imaginary (antisymmetric and thus Hermitian) at this order. Since the tree-level hard functions are real, the imaginary constant piece of the soft function at two loops is not relevant at the accuracy with which we work in this paper. However, the scale dependent part does contribute and is already predicted in the imaginary part of the soft anomalous dimension in eq. (4.3).

According to [207], the double real contribution is dipole-like and is completely incorporated in $\mathbf{S}_{\text{dip}}$. Therefore, we only need to calculate the real-virtual contribution. To this

JHEP09(2024)072

end, we make use of the tree-level and one-loop soft-gluon currents in [208],

$$\mathbf{J}_a^{(0)\mu}(q) = \sum_i \mathbf{T}_i^a \frac{p_i^\mu}{p_i \cdot q} \tag{4.13}$$

$$\begin{aligned}\mathbf{J}_a^{(1)\mu}(q,\epsilon) = &-\frac{1}{16\pi^2}\,\frac{1}{\epsilon^2}\,\frac{\Gamma^3(1-\epsilon)\,\Gamma^2(1+\epsilon)}{\Gamma(1-2\epsilon)} \\ &\times i\,f^{abc}\sum_{i\neq j}\mathbf{T}_i^b\,\mathbf{T}_j^c\left(\frac{p_i^\mu}{p_i\cdot q}-\frac{p_j^\mu}{p_j\cdot q}\right)\left[\frac{4\pi\,p_i\cdot p_j\,e^{-i\pi\lambda_{ij}}}{2(p_i\cdot q)\,(p_j\cdot q)\,e^{-i\pi\lambda_{iq}}\,e^{-i\pi\lambda_{jq}}}\right]^\epsilon\end{aligned} \tag{4.14}$$

where $\lambda_{AB} = +1$ if A and B are both incoming or outgoing, and $\lambda_{AB} = 0$ otherwise. The real-virtual integrand is [208],

$$\begin{aligned}&\mathbf{J}_\mu^{(0)}(q)\cdot\mathbf{J}^{(1)\mu}(q,\epsilon) + \text{h.c.} \\ &\quad= -\frac{1}{4\pi^2}\frac{(4\pi)^\epsilon}{\epsilon^2}\frac{\Gamma^3(1-\epsilon)\Gamma^2(1+\epsilon)}{\Gamma(1-2\epsilon)}\Bigg\{C_A\cos(\pi\epsilon)\sum_{i,j}{}'\left[\mathcal{S}_{ij}(q)\right]^{1+\epsilon}(\mathbf{T}_i\cdot\mathbf{T}_j) \\ &\qquad - 2i\sin(\pi\epsilon)\sum_{i,j,k}{}'\mathcal{S}_{ki}(q)\left[\mathcal{S}_{ij}(q)\right]^\epsilon(\lambda_{ij}-\lambda_{iq}-\lambda_{jq})\,(if^{abc})\,\mathbf{T}_k^a\mathbf{T}_i^b\mathbf{T}_j^c\Bigg\}.\end{aligned} \tag{4.15}$$

The dependence on whether partons are incoming or outgoing is encoded in λ,

$$\lambda_{ij}-\lambda_{iq}-\lambda_{jq} = 1 \text{ (i, j both incoming)}, \qquad -1 \text{ (otherwise)}. \tag{4.16}$$

The summation $\sum'$ stands for the sum over the different values of the indices. The soft eikonal function is defined as

$$\mathcal{S}_{ij}(q) = \frac{p_i\cdot p_j}{2\,(p_i\cdot q)\,(p_j\cdot q)} = \frac{s_{ij}}{s_{iq}s_{jq}}\,. \tag{4.17}$$

As discussed above, here we will focus on the three Wilson-line contribution which is represented as the last line of eq. (4.15).

Notice that only the imaginary part of the one-loop soft-gluon current survives in the tripole contribution (last line of eq. (4.15)). According to [53], this imaginary part is exactly the Glauber contribution. Therefore, we see that the tripole contribution at $\mathcal{O}(\alpha_s^2)$ in the soft function is purely from Glaubers. This is quite interesting since it is very different from the case for the dipole soft function, where Glauber effects only start to contribute at $\mathcal{O}(\alpha_s^3)$.

We now perform the calculation for the tripole contribution to the TEEC soft function with four Wilson lines. Making use of color conservation

$$\mathbf{T}_1+\mathbf{T}_2+\mathbf{T}_3+\mathbf{T}_4 = 0\,, \tag{4.18}$$

the color structure of the three-parton correlation can be reduced to $f^{abc}\mathbf{T}_1^a\mathbf{T}_2^b\mathbf{T}_3^c$. For example,

$$\begin{aligned}f^{abc}\mathbf{T}_1^a\mathbf{T}_2^b\mathbf{T}_4^c &= -f^{abc}\mathbf{T}_1^a\mathbf{T}_2^b\mathbf{T}_3^c - f^{abc}\mathbf{T}_1^a\mathbf{T}_2^b\mathbf{T}_1^c - f^{abc}\mathbf{T}_1^a\mathbf{T}_2^b\mathbf{T}_2^c \\ &= -f^{abc}\mathbf{T}_1^a\mathbf{T}_2^b\mathbf{T}_3^c\,,\end{aligned} \tag{4.19}$$

where we have used the relation

$$[\mathbf{T}_k^a,\mathbf{T}_j^b] = i\delta_{kj}f^{abc}\mathbf{T}_k^c\,. \tag{4.20}$$

JHEP09(2024)072

We define

$$I_{ijk} = \mathcal{S}_{ki}(q)\left[\mathcal{S}_{ij}(q)\right]^{\epsilon} . \tag{4.21}$$

The soft integrand becomes

$$\begin{aligned} & f_{abc}\sum_{i,j,k}{}'\mathbf{T}_k^a\mathbf{T}_i^b\mathbf{T}_j^c\ \mathcal{S}_{ki}(q)\left[\mathcal{S}_{ij}(q)\right]^{\epsilon}(\lambda_{ij}-\lambda_{iq}-\lambda_{jq}) \\ &= f^{abc}\mathbf{T}_1^a\mathbf{T}_2^b\mathbf{T}_3^c\big\{I_{123}-I_{124}+I_{132}-I_{134}-I_{142}+I_{143}-I_{213}+I_{214} \\ &\quad -I_{231}+I_{234}+I_{241}-I_{243}-I_{312}+I_{314}+I_{321}-I_{324}-I_{341}+I_{342} \\ &\quad +I_{412}-I_{413}-I_{421}+I_{423}+I_{431}-I_{432}\big\} . \end{aligned} \tag{4.22}$$

The rapidity divergences cancel separately in each term of the form $I_{ijk} - I_{jik}$, giving rise to a rapidity finite result. The phase space integrals can be performed straightforwardly. The final result is

$$\mathbf{S}_{\text{tri}}^{\text{bare}} = if^{abc}\mathbf{T}_1^a\mathbf{T}_2^b\mathbf{T}_3^c\, S_{\text{tri}}^{\text{bare}} = \left(\frac{\alpha_s}{4\pi}\right)^2 f^{abc}\mathbf{T}_1^a\mathbf{T}_2^b\mathbf{T}_3^c\,\ln\frac{\hat{t}}{\hat{u}}\left(\frac{b_y^2\mu^2}{4e^{-2\gamma_E}}\right)^{2\epsilon}\frac{8\pi}{3}\left(\frac{6}{\epsilon^2}+\pi^2+\mathcal{O}(\epsilon)\right) . \tag{4.23}$$

Notice that the color factor $f^{abc}\mathbf{T}_1^a\mathbf{T}_2^b\mathbf{T}_3^c$ is a purely imaginary matrix once the color basis is specified. The divergent terms appearing in this result can be predicted by the RG equation with the imaginary part of the anomalous dimensions in eq. (4.3).

We can also obtain the result for the TEEC soft function with three Wilson lines, which is relevant for $W/Z/\gamma$+jet. In that case, using the color conservation identity

$$\mathbf{T}_1+\mathbf{T}_2+\mathbf{T}_3 = 0 , \tag{4.24}$$

we clearly see that the tripole contribution vanishes due to the antisymmetry of f^{abc},

$$\mathbf{S}_{\text{tri}}^{\text{bare}}\Big|_{\text{Three Wilson Lines}} = 0 . \tag{4.25}$$

It would be interesting to understand whether or not a tripole contribution can contribute at higher perturbative orders.

In summary, this calculation explicitly shows that to two loops, the soft function is purely dipole for the two and three Wilson line soft functions, and for the four Wilson line soft function, there is a purely imaginary contribution.

4.4 Summary and discussion

We can summarize our one and two loop calculations as follows. The TEEC soft function has the perturbative expansion

$$\mathbf{S}(b_y, y^*, \mu, \nu) = \mathbf{1} + \frac{\alpha_s}{4\pi}\mathbf{S}^{(1)}(y^*, L_b, L_\nu) + \left(\frac{\alpha_s}{4\pi}\right)^2\mathbf{S}^{(2)}(y^*, L_b, L_\nu) + \mathcal{O}(\alpha_s^3) , \tag{4.26}$$

JHEP09(2024)072

with

$$\mathbf{S}^{(1)}(y^*, L_b, L_\nu) = -\sum_{i<j} (\mathbf{T}_i \cdot \mathbf{T}_j)\, S_\perp^{(1)}\left(L_b, L_\nu + \ln\frac{n_i \cdot n_j}{2}\right),$$

$$\mathbf{S}^{(2)}(y^*, L_b, L_\nu) = -\sum_{i<j} (\mathbf{T}_i \cdot \mathbf{T}_j)\, S_\perp^{(2)}\left(L_b, L_\nu + \ln\frac{n_i \cdot n_j}{2}\right) + \frac{1}{2!}\left(\mathbf{S}^{(1)}(y^*, L_b, L_\nu)\right)^2 + i f^{abc} \mathbf{T}_1^a \mathbf{T}_2^b \mathbf{T}_3^c\, S_{\rm tri}(y^*, L_b)\,. \tag{4.27}$$

Here $S_\perp^{(n)}(L_b, L_\nu)$ is the n-loop TMD soft function for color-singlet production at hadron colliders, and $S_{\rm tri}(y^*, L_b)$ is the purely imaginary tripole contribution calculated in eq. (4.23).

Our calculation also explicitly shows that at least to two loops, the color non-diagonal rapidity anomalous dimension, $\boldsymbol{\gamma}_X$, vanishes. This is guaranteed by rescaling invariance, $n_i \to e^{\lambda_i} n_i$, but is a non-trivial check on our calculation. We note that the consistency of the factorization formula, which is derived from demanding the rapidity scale independence of the cross section implies that $\boldsymbol{\gamma}_X = 0$ at all orders. This is a highly non-trivial statement, since at three loops there is a scaling invariant cross ratio $n_1{\cdot}n_3\, n_2{\cdot}n_4/(n_1{\cdot}n_2\, n_3{\cdot}n_4) = (1-\tanh y^*)^2/4$. If it is indeed true that $\boldsymbol{\gamma}_X = 0$, then we believe that there should be some argument for this fact purely at the level of the soft function definition. On the other hand, if $\boldsymbol{\gamma}_X \neq 0$, then this would indicate an explicit violation of factorization.

We note that one must be careful in what is meant by the soft function when discussing potential violations of factorization. In particular, it is normally assumed that Glauber contributions can simply be absorbed into the directions of Wilson lines (or proven in certain cases such as q_T). In the present case of the TEEC, where this is not expected to be true, one should probably work with the true soft function, defined by removing the Glauber zero-bin

$$S = \tilde{S} - S^{(G)}\,, \tag{4.28}$$

where $\tilde{S}$ denotes the naive soft function, and $S^{(G)}$ denotes is Glauber zero-bin [53]. Once this Glauber zero-bin contribution is removed, we expect that the naive factorization formula is not-violated. We are therefore led to the following conjecture

Rapidity dipole conjecture. The rapidity anomalous dimension for a soft function with Wilson lines in distinct directions n_i, is dipole to all loop order once the Glauber zero-bin is performed.

It would be extremely interesting to prove or disprove this statement, and we believe that it would improve our understanding of rapidity factorization with multiple collinear directions, for which little is known. This motivates a direct calculation of the TEEC soft function at three loops, as well as a better understanding of rapidity regularization for multi-Wilson line soft functions.

Finally, along the lines of [142, 193, 194], it will be important to better understand the all orders structure of rapidity anomalous dimensions for multi-Wilson line soft functions, perhaps by relating them to standard virtuality (μ) anomalous dimensions. (For other recent work understanding relations between anomalous dimensions defined by Wilson lines, see [209]). It would be interesting to obtain the rapidity anomalous dimension for multi-Wilson line soft functions in a similar manner, perhaps from some self crossing limit of a more complicated Wilson loop structure (see e.g. [210]).

JHEP09(2024)072

5 Color evolution at N^{3}LL

The beam and jet functions are color singlets, and their renormalization group evolution structure is standard. The most complicated aspect of the renormalization at N^{3}LL is the non-trivial color evolution of the hard and soft functions. Since this is applicable to any dijet soft function, and has not previously been presented at N^{3}LL accuracy, we discuss it in some detail with the hope that it will be useful more generally.

5.1 Hard and soft function anomalous dimensions

The soft function is a matrix in color space, and satisfies the RG equation

$$\frac{d\mathbf{S}}{d\ln\mu^2} = \frac{1}{2}\left(\mathbf{\Gamma}_S^\dagger \cdot \mathbf{S} + \mathbf{S}\cdot\mathbf{\Gamma}_S\right). \tag{5.1}$$

The anomalous dimension $\mathbf{\Gamma}_S$ takes the form given in eq. (4.3), which we repeat here for convenience [196–199]

$$\mathbf{\Gamma}_S = \sum_{i<j} \mathbf{T}_i\cdot\mathbf{T}_j\gamma_{\rm cusp}\ln\frac{\sigma_{ij}\nu^2\, n_i\cdot n_j - i0}{2\mu^2} - \sum_i \frac{c_i}{2}\gamma_s\mathbf{1} - \boldsymbol{\gamma}_{\rm quad}\,. \tag{5.2}$$

Here $\sigma_{ij} = -1$ if both i and j are incoming or outgoing, and $\sigma_{ij} = 1$ otherwise. ν is the rapidity scale, and $c_i = C_F$ or C_A is the Casimir of the parton i. Here $\gamma_{\rm cusp}$ is the cusp anomalous dimension [200], γ_s is the threshold soft anomalous dimension [201] and $\boldsymbol{\gamma}_{\rm quad}$ is the anomalous dimension for quadrupole color and kinematic entanglement, which first appears at three loops [104, 105]. Here we use the color space notation of [177]. The quadrupole anomalous dimension is universal (matter independent) [211], and can be written as a function of the conformal cross ratios. For extensive earlier work on its structure, see [197–199, 211–228], and for a detailed discussion summarizing the complete set of known results and their consistency, see [229].

To our knowledge, the quadrupole term in the anomalous dimension matrix has not yet entered into a physical observable. The quadrupole part of the soft anomalous dimension can be written as a sum of two terms

$$\Delta = 16(\mathbf{\Delta}_4^{(3)} + \mathbf{\Delta}_3^{(3)})\,. \tag{5.3}$$

In [105] it was shown in detail how to analytically continue the functions appearing in the quadrupole anomalous dimension to the physical region. However, in [230], an analytically continued form was given for $13 \to 24$ kinematics ($u = -s - t > 0$), which is sufficient for our purposes. Here we use the results of [230].

Restricting the general form of the quadrupole anomalous dimension to four external partons, for $\mathbf{\Delta}_3^{(3)}$, we have

$$\mathbf{\Delta}_3^{(3)} = -C\, f_{abe}f_{cde} \sum_{\substack{i=1\ldots4\\ 1\le j<k\le4\\ j,k\neq i}} \left\{\mathbf{T}_i^a, \mathbf{T}_i^d\right\}\mathbf{T}_j^b\mathbf{T}_k^c\,, \tag{5.4}$$

JHEP09(2024)072

or very explicitly

$$\begin{aligned}\boldsymbol{\Delta}_3^{(3)} = -C\, f_{abe} f_{cde} \Big[& \Big\{\mathbf{T}_1^a, \mathbf{T}_1^d\Big\} (\mathbf{T}_2^b \mathbf{T}_3^c + \mathbf{T}_2^b \mathbf{T}_4^c + \mathbf{T}_3^b \mathbf{T}_4^c) \\ & + \Big\{\mathbf{T}_2^a, \mathbf{T}_2^d\Big\} (\mathbf{T}_1^b \mathbf{T}_3^c + \mathbf{T}_1^b \mathbf{T}_4^c + \mathbf{T}_3^b \mathbf{T}_4^c) \\ & + \Big\{\mathbf{T}_3^a, \mathbf{T}_3^d\Big\} (\mathbf{T}_1^b \mathbf{T}_2^c + \mathbf{T}_1^b \mathbf{T}_4^c + \mathbf{T}_2^b \mathbf{T}_4^c) \\ & + \Big\{\mathbf{T}_4^a, \mathbf{T}_4^d\Big\} (\mathbf{T}_1^b \mathbf{T}_2^c + \mathbf{T}_1^b \mathbf{T}_3^c + \mathbf{T}_2^b \mathbf{T}_3^c) \Big] , \end{aligned} \tag{5.5}$$

where the constant C is given by

$$C = \zeta_5 + 2\zeta_3\zeta_2 \,. \tag{5.6}$$

For the analytic continuation of $\boldsymbol{\Delta}_4^{(3)}$, we use the form given in [230]

$$\boldsymbol{\Delta}_4^{(3)} = \frac{1}{4}\, f_{abe} f_{cde} \Big[\mathbf{T}_1^a \mathbf{T}_2^b \mathbf{T}_3^c \mathbf{T}_4^d\, \mathcal{S}(x) + \mathbf{T}_4^a \mathbf{T}_1^b \mathbf{T}_2^c \mathbf{T}_3^d\, \mathcal{S}(1/x) \Big], \tag{5.7}$$

where

$$\begin{aligned} \mathcal{S}(x) = {} & 2H_{-3,-2} + 2H_{-2,-3} - 2H_{-3,-1,-1} + 2H_{-3,-1,0} - 2H_{-2,-2,-1} + 2H_{-2,-2,0} - 2H_{-2,-1,-2} \\ & - H_{-1,-2,-2} - H_{-1,-1,-3} + 4H_{-2,-1,-1,-1} - 2H_{-2,-1,-1,0} - H_{-1,-2,-1,0} - H_{-1,-1,-2,0} \\ & + \zeta_3 H_{-1,-1} + 4\zeta_3\zeta_2 - \zeta_5 + \zeta_2(6H_{-3} - 10H_{-2,-1} + 6H_{-2,0} - H_{-1,-2} - H_{-1,-1,0}) \\ & + i\pi \Big[2H_{-3,-1} - 2H_{-3,0} + 2H_{-2,-2} - 4H_{-2,-1,-1} + 2H_{-2,-1,0} - 2H_{-2,0,0} + H_{-1,-2,0} \\ & + H_{-1,-1,0,0} + \zeta_2(3H_{-1,-1} - 4H_{-2}) - \zeta_3 H_{-1} \Big] . \end{aligned} \tag{5.8}$$

Here H are harmonic polylogarithms (HPLs), and the standard convention for the weights has been followed. The argument of the HPLs has been suppressed, and is $x = t/s$. This result contains explicit factors of $i\pi$ that are generated by the analytic continuation. While they do not contribute to the cross section at the order that we work, they would be interesting to understand from the perspective of Glaubers. We leave this to future work.

At N^{3}LL, we also need the cusp anomalous dimension at four loops [110]. Its value, as well as the value of all other anomalous dimensions required to derive the N^{3}LL result for the TEEC, are provided in appendix A.1.

5.2 Solving color evolution equations to N^{3}LL

The anomalous dimensions of the hard function in eq. (3.36) can be decomposed as the sum of a diagonal matrix and a non-diagonal matrix,

$$\boldsymbol{\Gamma}_H = \Gamma_h^D(\alpha_s, \mu)\mathbf{1} + \boldsymbol{\gamma}_h(\alpha_s) \,, \tag{5.9}$$

where $\boldsymbol{\gamma}_h$ is the non-diagonal matrix contribution, which can be written as

$$\boldsymbol{\gamma}_h = \frac{\alpha_s}{4\pi}\boldsymbol{\gamma}_0^h + \left(\frac{\alpha_s}{4\pi}\right)^2 \boldsymbol{\gamma}_1^h + \left(\frac{\alpha_s}{4\pi}\right)^3 \boldsymbol{\gamma}_2^h + \cdots . \tag{5.10}$$

JHEP09(2024)072

The solution to the hard function RG equation is

$$\boldsymbol{H}(\mu) = \boldsymbol{U}(\mu_h, \mu)\ \boldsymbol{H}(\mu_h)\ \boldsymbol{U}^\dagger(\mu_h, \mu)\,, \tag{5.11}$$

with

$$\boldsymbol{U}(\mu_h, \mu) = \exp\left[\int_{\mu_h}^{\mu} \frac{d\bar{\mu}}{\bar{\mu}} \Gamma_h^D(\alpha_s(\bar{\mu}), \bar{\mu})\right] \boldsymbol{u}(\mu_h, \mu). \tag{5.12}$$

The factor $\int_{\mu_h}^{\mu} \frac{d\bar{\mu}}{\bar{\mu}} \Gamma_h^D(\alpha_s(\bar{\mu}), \bar{\mu})$ includes the evolution similar to a color singlet state. The non-trivial color evolution is included in $\boldsymbol{u}$ which obeys the differential equations

$$\begin{aligned} \frac{d}{d\ln\mu}\boldsymbol{u}(\mu_h, \mu) &= \boldsymbol{\gamma}_h(\alpha_s(\mu))\boldsymbol{u}(\mu_h, \mu)\,, \\ \frac{d}{d\ln\mu_h}\boldsymbol{u}(\mu_h, \mu) &= -\boldsymbol{u}(\mu_h, \mu)\boldsymbol{\gamma}_h(\alpha_s(\mu_h))\,. \end{aligned} \tag{5.13}$$

The solution to these equations is

$$\boldsymbol{u}(\mu_h, \mu) = \mathcal{P} \exp\left[\int_{\alpha_s(\mu_h)}^{\alpha_s(\mu)} \frac{d\alpha}{\beta(\alpha)} \boldsymbol{\gamma}_h(\alpha)\right]\,, \tag{5.14}$$

where $\mathcal{P}$ denotes the ordering in the coupling constant with the scale in the coupling increasing from left to right. The ordering operator is necessary when $[\boldsymbol{\gamma}_h(\alpha_1), \boldsymbol{\gamma}_h(\alpha_2)] \neq 0$. Here we will give explicit expressions for the $\mathbf{u}$ matrix at NLL, NNLL and N^{3}LL.

At NLL the $\mathbf{u}$ matrix is given by

$$\boldsymbol{u}_{\rm NLL}(\mu_h, \mu) = \boldsymbol{V}\ \left(\frac{\alpha_s(\mu)}{\alpha_s(\mu_h)}\right)^{-\frac{\gamma_{\rm D}^0}{2\beta_0}} \boldsymbol{V}^{-1}\,, \tag{5.15}$$

where $\boldsymbol{V}$ is the matrix that diagonalizes the LO anomalous dimension

$$\boldsymbol{\gamma}_D^0 = \boldsymbol{V}^{-1}\ \boldsymbol{\gamma}_0^h\ \boldsymbol{V}\,. \tag{5.16}$$

Higher order QCD corrections can be included by expressing them in terms of $\mathbf{u}_{\rm NLL}$ as [231]

$$\boldsymbol{u}(\mu_h, \mu) = \boldsymbol{K}(\mu)\boldsymbol{u}_{\rm NLL}(\mu_h, \mu)\boldsymbol{K}^{-1}(\mu_h)\,. \tag{5.17}$$

From eq. (5.13), the differential equation for the matrix $\mathbf{K}$ up to NNLO is

$$\begin{aligned} &\beta(\alpha_s(\mu))\frac{d}{d\alpha_s(\mu)}\boldsymbol{K}(\alpha_s(\mu)) - \frac{\beta(\alpha_s(\mu))}{2\alpha_s(\mu)\beta_0}\boldsymbol{K}(\alpha_s(\mu))\boldsymbol{\gamma}_0^h \\ &\qquad = \frac{\alpha_s(\mu)}{4\pi}\boldsymbol{\gamma}_0^h\boldsymbol{K}(\mu) + \left(\frac{\alpha_s(\mu)}{4\pi}\right)^2 \boldsymbol{\gamma}_1^h\boldsymbol{K}(\mu) + \left(\frac{\alpha_s(\mu)}{4\pi}\right)^3 \boldsymbol{\gamma}_2^h\boldsymbol{K}(\mu)\,. \end{aligned} \tag{5.18}$$

Defining the perturbative expansion of $\boldsymbol{K}$ as

$$\boldsymbol{K} = \mathbf{1} + \frac{\alpha_s(\mu)}{4\pi}\boldsymbol{K}_0 + \left(\frac{\alpha_s(\mu)}{4\pi}\right)^2 \boldsymbol{K}_1 + \cdots\,, \tag{5.19}$$

JHEP09(2024)072

we have

$$\boldsymbol{K}_0 + \frac{1}{2\beta_0}[\boldsymbol{\gamma}_0^h, \boldsymbol{K}_0] = \frac{\beta_1 \boldsymbol{\gamma}_0^h}{2\beta_0^2} - \frac{\boldsymbol{\gamma}_1^h}{2\beta_0}\,.$$
$$\boldsymbol{K}_1 + \frac{1}{4\beta_0}[\boldsymbol{\gamma}_0^h, \boldsymbol{K}_1] = \frac{1}{4\beta_0}\left(\frac{\beta_1}{\beta_0}\boldsymbol{\gamma}_0^h \boldsymbol{K}_0 - \boldsymbol{\gamma}_1^h \boldsymbol{K}_0 - \frac{\beta_1^2}{\beta_0^2}\boldsymbol{\gamma}_0^h + \frac{\beta_1}{\beta_0}\boldsymbol{\gamma}_1^h + \frac{\beta_2}{\beta_0}\boldsymbol{\gamma}_1^h - \boldsymbol{\gamma}_2^h\right). \tag{5.20}$$

Using eq. (5.16) we transform $\boldsymbol{K}$ into $\boldsymbol{S} = \boldsymbol{V}^{-1}\boldsymbol{K}\boldsymbol{V}$, and perturbatively expand $\boldsymbol{S}_i$ as

$$\boldsymbol{S} = \boldsymbol{1} + \frac{\alpha_s(\mu)}{4\pi}\boldsymbol{S}_0 + \left(\frac{\alpha_s(\mu)}{4\pi}\right)^2 \boldsymbol{S}_1 + \cdots\,. \tag{5.21}$$

The solution of eq. (5.20) is then given by

$$\boldsymbol{S}_{0,IJ} = \delta_{IJ}\frac{\beta_1}{2\beta_0^2}(\gamma_D^0)_{JJ} - \frac{(\boldsymbol{V}^{-1}\boldsymbol{\gamma}_1^h\boldsymbol{V})_{IJ}}{2\beta_0 + (\gamma_D^0)_{II} - (\gamma_D^0)_{JJ}}\,,$$
$$\boldsymbol{S}_{1,IJ} = \frac{\delta_{IJ}}{4\beta_0}\left(\frac{\beta_2}{\beta_0} - \frac{\beta_1^2}{\beta_2^2}\right)(\gamma_D^0)_{JJ}$$
$$+ \frac{1}{4\beta_0 + (\gamma_D^0)_{II} - (\gamma_D^0)_{JJ}}\left(\boldsymbol{V}^{-1}\left(\frac{\beta_1}{\beta_0}\boldsymbol{\gamma}_0^h\boldsymbol{K}_0 - \boldsymbol{\gamma}_1^h\boldsymbol{K}_0 + \frac{\beta_1}{\beta_0}\boldsymbol{\gamma}_1^h - \boldsymbol{\gamma}_2^h\right)\boldsymbol{V}\right)_{IJ}. \tag{5.22}$$

The expressions for the $\boldsymbol{u}$ matrices at NNLL and N^{3}LL are

$$\boldsymbol{u}_{\mathrm{NNLL}}(\mu_h,\mu) = \boldsymbol{V}\left(1 + \frac{\alpha_s(\mu)}{4\pi}\boldsymbol{S}_0\right)\left(\frac{\alpha_s(\mu)}{\alpha_s(\mu_h)}\right)^{-\frac{\gamma_{\mathrm{D}}^0}{2\beta_0}}\left(1 + \frac{\alpha_s(\mu_h)}{4\pi}\boldsymbol{S}_0\right)^{-1}\boldsymbol{V}^{-1}\,,$$
$$\boldsymbol{u}_{\mathrm{N^3LL}}(\mu_h,\mu) = \boldsymbol{V}\left(1 + \frac{\alpha_s(\mu)}{4\pi}\boldsymbol{S}_0 + \left(\frac{\alpha_s(\mu)}{4\pi}\right)^2\boldsymbol{S}_1\right)\left(\frac{\alpha_s(\mu)}{\alpha_s(\mu_h)}\right)^{-\frac{\gamma_{\mathrm{D}}^0}{2\beta_0}}$$
$$\times\left(1 + \frac{\alpha_s(\mu_h)}{4\pi}\boldsymbol{S}_0 + \left(\frac{\alpha_s(\mu_h)}{4\pi}\right)^2\boldsymbol{S}_1\right)^{-1}\boldsymbol{V}^{-1}\,. \tag{5.23}$$

These matrices allow for the resummation up to N^{3}LL for generic color mixing matrices, and we believe that they will prove useful in many future studies of event shapes at hadron colliders, or multi-jet event shapes in e^+e^- colliders.

6 Linearly polarized beam and jet functions

Another interesting feature of the TEEC which first appears at N^{3}LL, is the presence of linearly polarized jet and beam functions. Since the TEEC is measuring radiation perpendicular to the scattering plane formed by the hard process, the helicity of gluons in the jets or beams can lead to terms which have an azimuthal dependence as they are rotated through this plane. These are described by the linearly polarized beam and jet functions. Similar polarization effects in the collinear limit of the energy correlators were discussed in [232–234]. There the effect came from the presence of other detectors, instead of the plane of the hard scattering process. The matching coefficients for the gluonic TMD beam and fragmentation functions can be decomposed into tensor structures as

$$\mathcal{I}_{gi}^{\mu\nu}(\xi, b_\perp) = \frac{g_\perp^{\mu\nu}}{d-2}\mathcal{I}_{gi}(\xi, b_\perp) + \left(\frac{g_\perp^{\mu\nu}}{d-2} + \frac{b_\perp^\mu b_\perp^\nu}{b_T^2}\right)\mathcal{I}'_{gi}(\xi, b_\perp)\,. \tag{6.1}$$

JHEP09(2024)072

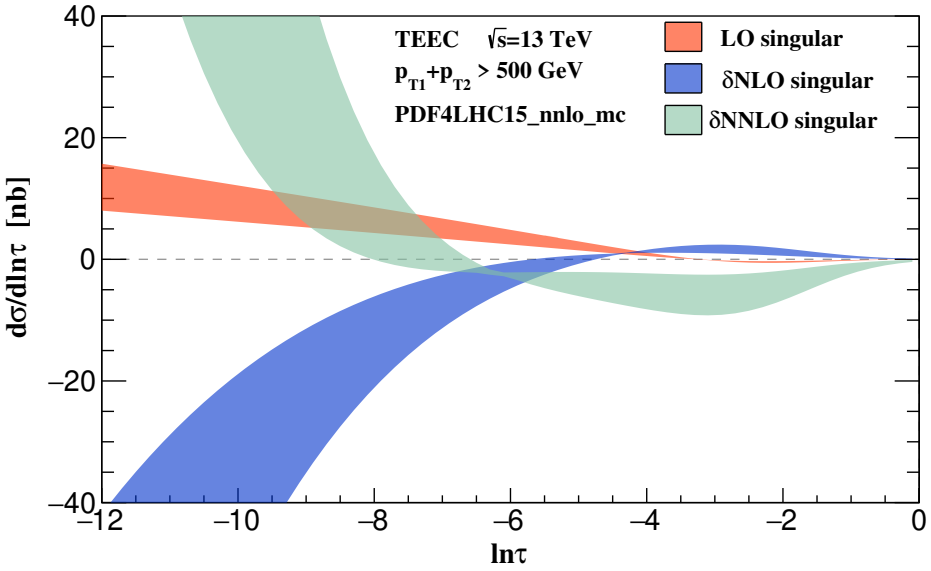

Figure 5. The fixed order singular behavior of the TEEC cross section at LO, NLO and NNLO derived using our factorization formula.

For a detailed discussion and NNLO calculation for both TMD beam functions and fragmentation functions in our regulator, see [116]. The one loop matching coefficients and the one-loop beam and jet functions for linearly polarized gluons are given in appendix A. Importantly, they are first non-zero at one loop, where they give finite results.

An interesting feature of the TEEC on dijets, is that the tree level hard scattering matrix elements are maximal helicity violating (MHV). Therefore, when contracted with a single linearly polarized jet or beam function, the result vanishes. One must either have two linearly polarized jet or beam functions, or a one-loop correction to the hard scattering matrix element to get a non-vanishing NMHV amplitude combined with a single linearly polarized beam or jet function. For a detailed discussion of the helicity structure of SCET hard matching coefficients, and explicit results, see [173]. This shows that for the TEEC on dijets, effects from linearly polarized beam and jet functions first enter as a constant at $\mathcal{O}(\alpha_s^2)$, namely at N^{3}LL. For this reason, they were not needed in our NNLL calculation [64]. This is in distinction to the case of the TEEC on $V+$ jets, or other related $V+$ jet observables [166, 167], where linearly polarized jet and beam functions enter at NNLL, since the hard function does not have an MHV structure.

It would be interesting to study the phenomenological impact of these linearly polarized terms in more detail. However, since the focus of this paper has been on the derivation of the factorization formula, we leave such studies to future work.

7 Fixed order singular behavior

In [64], we verified that our factorization formula correctly reproduced the singular behavior of the TEEC observable by comparing with numerical results obtained using NLOJET++ [235, 236] for all partonic channels. Here we can use our factorization formula, expanded to fixed

JHEP09(2024)072

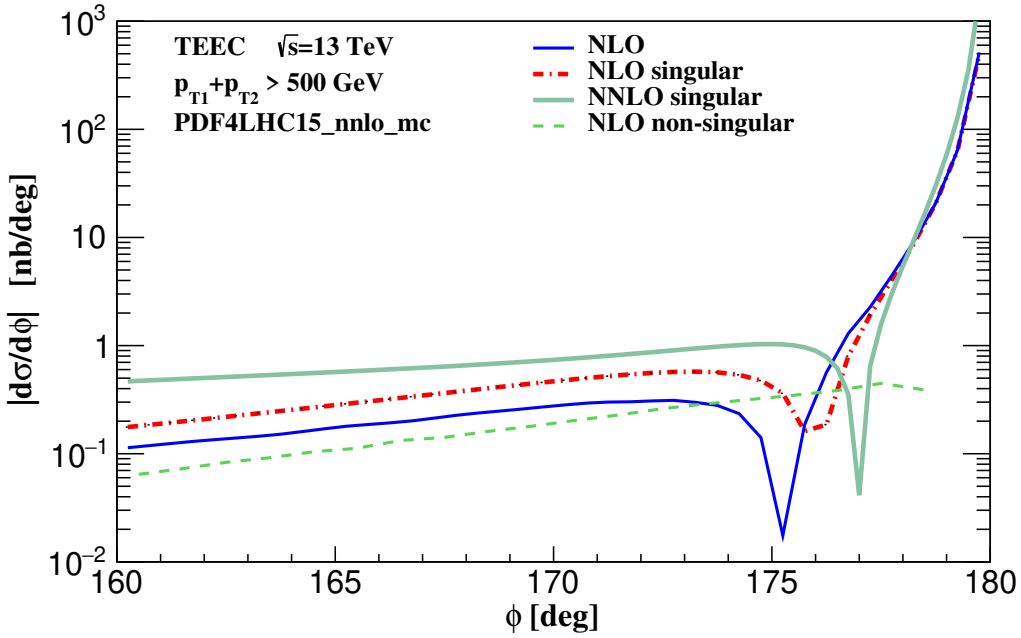

Figure 6. The singular behavior of the TEEC cross section at NLO and NNLO. At NLO, we also show the full result, as computed numerically using NLOJET++, as well as the non-singular contribution. It would be interesting to compare to the recent calculation of the TEEC at NNLO [56, 125], but this is beyond the scope of this paper.

order, to predict the NNLO singular behavior of the $pp \to 3$ jet cross section in the $\tau \to 0$ limit. For simplicity, we neglect the linearly polarized terms.

For our numerical results we consider the conditions of the LHC at $\sqrt{s} = 13\,\text{TeV}$. We select events with two leading jets having averaged jet $P_T \geq 250\,\text{GeV}$ and individual jet rapidity $|Y| < 2.5$, where the jets are defined using the anti-k_T algorithm [237] with $R = 0.4$. The TEEC is then computed on all particles with rapidity $|y| < 2.5$. For PDFs, we use the PDF4LHC15_nnlo_mc [238] parton distribution functions. We take $\alpha_s(M_Z) = 0.118$.

In figure 5 we show the singular structure at LO, NLO, and NNLO on a logarithmic scale, and in figure 6 on a linear scale. In figure 6, we also show the non-singular contributions (power corrections) at NLO. There has recently been progress in understanding the structure of the power corrections for q_T in color singlet production [239, 240] and the EEC [241, 242], and it would be interesting to extend this to the case of the TEEC. As mentioned above, the NNLO result is obtained under the assumption that there is no factorization violation at this order, namely that our factorization formula predicts the complete singular structure. While this remains to be proven, it is strongly suggested by previous work [44, 50].

8 Resummed results at N^{3}LL

Although the main focus of this paper has been on the derivation of the factorization formula, and the calculation of the relevant ingredients necessary for resummation at N^{3}LL level, here we provide illustrative numerical results to study the perturbative convergence. Ultimately, to provide a complete description of the TEEC, one should match to fixed order perturbative

JHEP09(2024)072

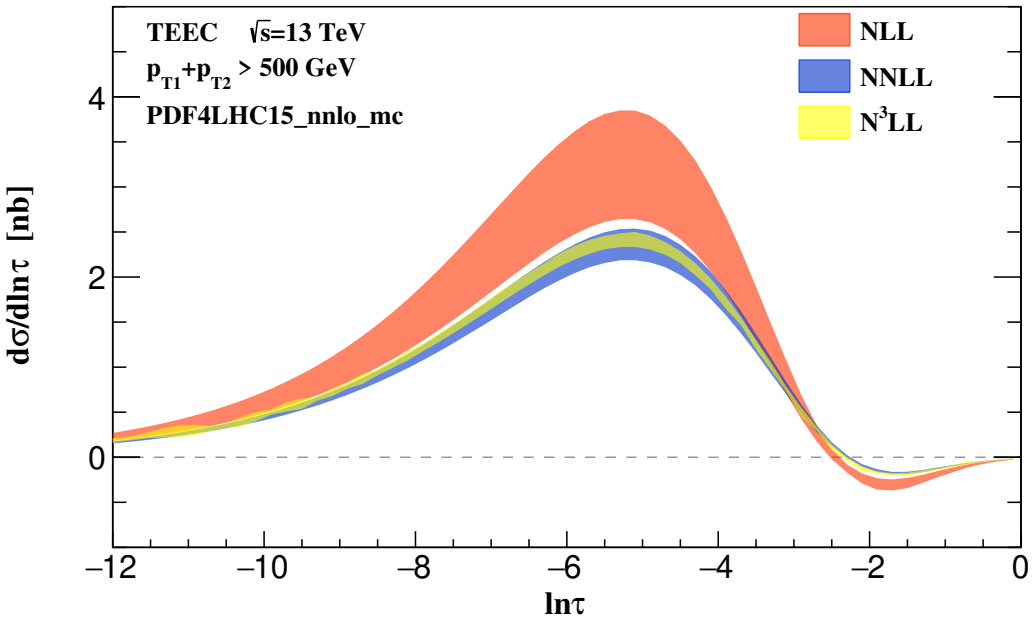

Figure 7. Resummed results for the TEEC at NLL, NNLL and N^{3}LL. Good perturbative convergence is observed. It will be particularly interesting to match the N^{3}LL result to the NNLO $pp \to 3$ jet fixed order calculation [125].

results. At N^{3}LL, one should match to the NNLO calculation of the three jet cross section. Remarkably, this has recently been achieved, and the NNLO calculation of the three jet cross section [125], has enabled the NNLO calculation of hadron collider dijet event shapes [56]. This provides the perturbative accuracy necessary to match our resummed calculation to fixed order perturbation theory. Unfortunately, performing this matching is beyond the scope of the current paper, since these results just became available. Therefore, we settle for illustrating the resummed singular results. Since we are not performing the full matching, for simplicity, we do not include the linearly polarized contributions. These are straightforward to include, and will be incorporated in phenomenological results in future work.

In figure 7 we present the resummed results at NLL, NNLL and N^{3}LL, extending the results of [64]. The scale uncertainty bands are constructed by varying all the scales by a factor of 1/2 or 2 around their canonical values,

$$\mu_h = Q\,, \quad \mu_j = b_0/b_y\,, \quad \mu_s = b_0/b_y\,, \quad \nu_j = Q\,, \qquad \nu_s = b_0/b_y\,, \tag{8.1}$$

where subscripts h, j, s denote hard, jet, soft respectively. In order to avoid the Landau pole, we replace b_y by $b_y/\sqrt{1+b_y^2/b_{\rm max}^2}$ with $b_{\rm max} = 2\,{\rm GeV}^{-1}$. Good perturbative convergence is observed from NNLL to N^{3}LL. The fact that the cross section goes negative as $\tau \to 1$ is unphysical, and is a result of the fact that one should match to the full fixed order result. This represents the first example of a dijet event shape resummed to this accuracy at the LHC.

9 Conclusions

Despite their interest for understanding QCD, hadron collider event shapes with final state jets are notoriously difficult to calculate, and have so far resisted higher order resummation.

JHEP09(2024)072

In this paper we have derived a factorization formula for the TEEC in the back-to-back limit, and shown that it exhibits a remarkable theoretical simplicity. This simplicity allowed us to perform its resummation to N^{3}LL, greatly extending the previous highest order NLL resummation. Of particular interest, at N^{3}LL, we first encounter a contribution from the quadrupole anomalous dimension [104, 105], where the colors of all jets are entangled. This represents, to our knowledge, the first time it has appeared in a physical event shape observable. We also observe interesting contributions from linearly polarized gluons in both beam and jet functions.

We also introduced definitions of the TEEC observable for Drell-Yan, and $W/Z/\gamma+$ jet processes, and showed that they all fit into the same framework and can all be computed to N^{3}LL accuracy. The TEEC therefore provides a natural generalization of transverse momentum observable to states with jets, making it a valuable probe of TMD dynamics at hadron colliders.

A complete description of the TEEC description requires a number of further ingredients, beyond the resummation of singular contributions presented here. First, we would like to be able to match to the fixed order $2 \to 3$ jet amplitudes at NNLO, which have recently become available [56, 125, 243–245]. Second, it will be important to understand the structure of non-perturbative corrections to the TEEC in the back-to-back limit. Non-perturbative corrections have been studied for the EEC [31, 84, 246–248], and we believe that using our operator based definition, we can extend these studies to the TEEC.

It would be particularly interesting to measure the back-to-back limit of the TEEC precisely to study the resummation effects calculated in this paper in data. Recent measurements of the TEEC have used jets instead of hadrons [9] to achieve increased precision. It would be interesting to understand if this measurement could be done precisely on hadrons. On the theory side, there has been significant progress in understand the incorporation of tracking information [249–254] in perturbative calculations. This allows the calculation of the track based TEEC, which perhaps could be measured more precisely.

Finally, it will be important to understand potential factorization violating effects. We have shown that for the TEEC the contributions of the underlying event are quite small, and are easily accounted for by adding an energy distribution that is uniform in the azimuthal angle. We believe that perturbative factorization violation will occur at N^{4}LL, and it would be interesting to prove this. In particular, it will be interesting to compute the TEEC soft function at N^{3}LO to see if it has a quadrupole rapidity anomalous dimension, which would provide a concrete illustration of the violation of factorization. We are also optimistic that due to the simple perturbative structure of the TEEC observable, it can provide a playground for understanding perturbative factorization violation, and we have highlighted how the fact that the TEEC can be defined on a number of distinct final states may facilitate this understanding. We intend to pursue these directions in future work.

Acknowledgments

We would like to thank Thomas Gehrmann, Xuan Chen, Duff Neill, Wouter Waalewijn, Matt LeBlanc, Jennifer Roloff, Ben Nachman and Iain Stewart for useful discussions. I.M and H.X.Z would like to thank the MITP for hospitality while portions of this work were

JHEP09(2024)072

performed. A.G. was supported by the U.S. Department of Energy under contract number DE-SC0011090. H.T.L. is supported by the National Science Foundation of China under grant Nos. 12275156 and 12321005. I.M was supported by start-up funds from Yale University. H.X.Z was supported by the National Science Foundation of China under grant No.11975200 and the Asian Young Scientist Fellowship.

A Summary of perturbative ingredients

In this appendix, we summarize the perturbative ingredients entering our calculation.

A.1 Anomalous dimensions

We denote our anomalous dimensions as $\gamma[\alpha_s, \ldots]$, with the dots representing potential dependence on kinematical variables. We expand them perturbatively in α_s as,

$$\gamma[\alpha_s, \ldots] = \sum_{n=0}^{\infty} \left(\frac{\alpha_s}{4\pi}\right)^{n+1} \gamma_n[\ldots] \,. \tag{A.1}$$

The QCD beta function $\beta[\alpha_s] = -2\alpha_s \sum_{n=0}(\alpha_s/(4\pi))^{n+1}\beta_n$ through to three loops is given by [255, 256]

$$\begin{aligned}
\beta_0 &= \frac{11C_A}{3} - \frac{2n_f}{3} \,, \\
\beta_1 &= \frac{34C_A^2}{3} - \frac{10C_A n_f}{3} - 2C_F n_f \,, \\
\beta_2 &= \frac{2857C_A^2}{54} + C_F^2 n_f - \frac{205C_F C_A n_f}{18} - \frac{1415C_A^2 n_f}{54} + \frac{11C_F n_f^2}{9} + \frac{79C_A n_f^2}{54} \,, \\
\beta_3 &= \frac{149753}{6} + 3564\zeta_3 - \left(\frac{6508\zeta_3}{27} + \frac{1078361}{162}\right) n_f + \left(\frac{6472\zeta_3}{81} + \frac{50065}{162}\right) n_f^2 + \frac{1093 n_f^3}{729} \,.
\end{aligned} \tag{A.2}$$

The cusp anomalous dimension is given through to four loops by [107–110, 200, 257]

$$\begin{aligned}
\gamma_0^{\text{cusp}} &= 4 \,, \\
\gamma_1^{\text{cusp}} &= C_A \left(\frac{268}{9} - 8\zeta_2\right) - \frac{40 n_f}{9} \,, \\
\gamma_2^{\text{cusp}} &= C_A^2 \left(-\frac{1072\zeta_2}{9} + \frac{88\zeta_3}{3} + 88\zeta_4 + \frac{490}{3}\right) + C_A n_f \left(\frac{160\zeta_2}{9} - \frac{112\zeta_3}{3} - \frac{836}{27}\right) \\
&\quad + C_F n_f \left(32\zeta_3 - \frac{110}{3}\right) - \frac{16 n_f^2}{27} \,, \\
\gamma_{3,q}^{\text{cusp}} &= 15526.5 - 3878.93\, n_f + 146.683\, n_f^2 + 2.454\, n_f^3 \,, \\
\gamma_{3,g}^{\text{cusp}} &= 13626.7 - 3904.67\, n_f + 146.683\, n_f^2 + 2.454\, n_f^3 \,.
\end{aligned} \tag{A.3}$$

The full analytic result can be found in [110]. Note that at four loops the Casimir scaling between quark and gluon cusp anomalous dimensions is broken. The quark and gluon anomalous dimensions through to three loops are [258–262]

$$\gamma_0^q = -3C_F \,,$$

JHEP09(2024)072

$$
\begin{aligned}
\gamma_1^q &= C_A C_F \left(-11\zeta_2 + 26\zeta_3 - \frac{961}{54}\right) + C_F^2 \left(12\zeta_2 - 24\zeta_3 - \frac{3}{2}\right) + C_F n_f \left(2\zeta_2 + \frac{65}{27}\right) , \\
\gamma_2^q &= -\frac{4880\pi^2\zeta_3}{81} + \frac{82072\zeta_3}{27} - \frac{15328\zeta_5}{9} - \frac{2066\pi^4}{405} - \frac{5062\pi^2}{81} - \frac{196621}{243} \\
&\quad + \left(-\frac{7472\zeta_3}{81} + \frac{68\pi^4}{1215} + \frac{4564\pi^2}{243} + \frac{36236}{729}\right) n_f + \left(-\frac{32\zeta_3}{81} - \frac{40\pi^2}{81} + \frac{9668}{2187}\right) n_f^2 , \\
\gamma_0^g &= -\beta_0 , \\
\gamma_1^g &= C_A^2 \left(\frac{11\zeta_2}{3} + 2\zeta_3 - \frac{692}{27}\right) + C_A n_f \left(\frac{128}{27} - \frac{2\zeta_2}{3}\right) + 2C_F n_f , \\
\gamma_2^g &= -60\pi^2\zeta_3 + 1098\zeta_3 - 432\zeta_5 - \frac{319\pi^4}{10} + \frac{6109\pi^2}{18} - \frac{97186}{27} \\
&\quad + \left(\frac{460\zeta_3}{9} + \frac{107\pi^4}{45} - \frac{635\pi^2}{27} + \frac{59635}{162}\right) n_f + \left(-\frac{56\zeta_3}{9} + \frac{10\pi^2}{27} - \frac{1061}{486}\right) n_f^2 .
\end{aligned} \tag{A.4}
$$

The soft anomalous dimension up to three loops is [201]

$$
\begin{aligned}
\gamma_0^s &= 0 , \\
\gamma_1^s &= C_A \left(-\frac{808}{27} + \frac{22}{3}\zeta_2 + 28\zeta_3\right) + n_f \left(\frac{112}{27} - \frac{4}{3}\zeta_2\right) , \\
\gamma_2^s &= C_A^2 \left(-\frac{136781}{729} + \frac{12650}{81}\zeta_2 + \frac{1316}{3}\zeta_3 - 176\zeta_4 - 192\zeta_5 - \frac{176}{3}\zeta_3\zeta_2\right) \\
&\quad + C_A n_f \left(\frac{11842}{729} - \frac{2828}{81}\zeta_2 - \frac{728}{27}\zeta_3 + 48\zeta_4\right) \\
&\quad + C_F n_f \left(\frac{1711}{27} - 4\zeta_2 - \frac{304}{9}\zeta_3 - 16\zeta_4\right) + n_f^2 \left(\frac{2080}{729} + \frac{40}{27}\zeta_2 - \frac{112}{27}\zeta_3\right) .
\end{aligned} \tag{A.5}
$$

The rapidity anomalous dimension up to three loops is [106]

$$
\begin{aligned}
\gamma_0^r &= 0 , \\
\gamma_1^r &= C_A \left(-\frac{808}{27} + 28\zeta_3\right) + n_f \frac{112}{27} , \\
\gamma_2^r &= C_A^2 \left(-\frac{297029}{729} + \frac{6392}{81}\zeta_2 + \frac{12328}{27}\zeta_3 + \frac{154}{3}\zeta_4 - 192\zeta_5 - \frac{176}{3}\zeta_3\zeta_2\right) \\
&\quad + C_A n_f \left(\frac{62626}{729} - \frac{824}{81}\zeta_2 - \frac{904}{27}\zeta_3 + \frac{20}{3}\zeta_4\right) + n_f^2 \left(-\frac{1856}{729} - \frac{32}{9}\zeta_3\right) \\
&\quad + C_F n_f \left(\frac{1711}{27} - \frac{304}{9}\zeta_3 - 16\zeta_4\right) .
\end{aligned} \tag{A.6}
$$

A.2 Beam functions

The unpolarized TMD beam functions at one loop are given by

$$
\begin{aligned}
\mathcal{I}_{qq}(z, L_b, L_Q) &= \delta(1-z) + \left(\frac{\alpha_s}{4\pi}\right) \Big[C_F \left(-2L_b L_Q + 3L_b\right) \delta(1-z) - P_{0,\,qq}(z) L_b + 2C_F(1-z)\Big] \\
&\quad + \mathcal{O}(\alpha_s^2) , \\
\mathcal{I}_{qg}(z, L_b, L_Q) &= \left(\frac{\alpha_s}{4\pi}\right) \Big[2z(1-z) - P_{0,qg}(z) L_b\Big] + \mathcal{O}(\alpha_s^2) ,
\end{aligned}
$$

$$\mathcal{I}_{gq}(z, L_b, L_Q) = \left(\frac{\alpha_s}{4\pi}\right)\Big[- P_{0,\,gq}(z) L_b + 2C_F\, z\Big] + \mathcal{O}(\alpha_s^2)\,, \tag{A.7}$$

$$\mathcal{I}_{gg}(z, L_b, L_Q) = \delta(1-z) + \left(\frac{\alpha_s}{4\pi}\right)\Big[\left(-2C_A L_b L_Q + \beta_0 L_b\right)\delta(1-z) - P_{0,\,gg}(z) L_b\Big] + \mathcal{O}(\alpha_s^2)\,.$$

where $P_{0,ij}(z)$ are the LO splitting functions

$$\begin{aligned}
P_{0,qq}(z) &= C_F\left[3\delta(1-z) + \frac{4}{[1-z]_+} - 2(1+z)\right]\,,\\
P_{0,qg}(z) &= 1 - 2z + 2z^2\,,\\
P_{0,gq}(z) &= 2C_F\left[\frac{1+(1-z)^2}{z}\right]\,,\\
P_{0,gg}(z) &= 4C_A\left[\frac{z}{[1-z]_+} + \frac{1-z}{z} + z(1-z)\right] + \beta_0\delta(1-z)\,.
\end{aligned} \tag{A.8}$$

The complete two-loop results using the exponential regulator used in this paper can be found in [115, 116], and the three-loop results can be found in [138–141].

The linearly polarized beam functions at one loop are finite, and are given by

$$\begin{aligned}
\mathcal{I}'_{gq} &= \left(\frac{\alpha_s}{4\pi}\right) 4C_F \frac{1-x}{x} + \mathcal{O}(\alpha_s^2)\,,\\
\mathcal{I}'_{gg} &= \left(\frac{\alpha_s}{4\pi}\right) 4C_A \frac{1-x}{x} + \mathcal{O}(\alpha_s^2)\,.
\end{aligned} \tag{A.9}$$

A detailed discussion, and results of two loops can be found in [116].

A.3 Jet functions

The TEEC jet functions are given at one loop by [77]

$$\begin{aligned}
J_q(b_y, \mu, \nu) &= J_{\bar{q}}(b_y, \mu, \nu) = 1 + \left(\frac{\alpha_s}{4\pi}\right) C_F(-2L_b L_Q + 3L_b + 4 - 8\zeta_2) + \mathcal{O}(\alpha_s^2)\,,\\
J_g(b_y, \mu, \nu) &= 1 + \left(\frac{\alpha_s}{4\pi}\right)\left[-2C_A L_b L_Q + \beta_0 L_b + \left(\frac{65}{18} - 8\zeta_2\right) C_A - \frac{5}{18} n_f\right] + \mathcal{O}(\alpha_s^2)\,.
\end{aligned} \tag{A.10}$$

The complete two-loop results can be found in [115, 116], and the three-loop results in [139, 140].

The linearly polarized gluon jet function at one loop is finite, which is given by

$$J'_g(b_y, \mu, \nu) = \left(\frac{\alpha_s}{4\pi}\right)\left(\frac{C_A}{3} - \frac{N_f}{3}\right) + \mathcal{O}(\alpha_s^2)\,, \tag{A.11}$$

and results to two loops can be found in [116].

JHEP09(2024)072

References

[1] CMS collaboration, *First Measurement of Hadronic Event Shapes in pp Collisions at $\sqrt{s} = 7$ TeV*, *Phys. Lett. B* **699** (2011) 48 [arXiv:1102.0068] [INSPIRE].

[2] ATLAS collaboration, *Measurement of event shapes at large momentum transfer with the ATLAS detector in pp collisions at $\sqrt{s} = 7$ TeV*, *Eur. Phys. J. C* **72** (2012) 2211 [arXiv:1206.2135] [INSPIRE].

[3] ATLAS collaboration, *Measurement of charged-particle event shape variables in $\sqrt{s} = 7$ TeV proton-proton interactions with the ATLAS detector*, *Phys. Rev. D* **88** (2013) 032004 [arXiv:1207.6915] [INSPIRE].

[4] CMS collaboration, *Event Shapes and Azimuthal Correlations in Z + Jets Events in pp Collisions at $\sqrt{s} = 7$ TeV*, *Phys. Lett. B* **722** (2013) 238 [arXiv:1301.1646] [INSPIRE].

[5] CMS collaboration, *Study of Hadronic Event-Shape Variables in Multijet Final States in pp Collisions at $\sqrt{s} = 7$ TeV*, *JHEP* **10** (2014) 087 [arXiv:1407.2856] [INSPIRE].

[6] ATLAS collaboration, *Measurement of transverse energy-energy correlations in multi-jet events in pp collisions at $\sqrt{s} = 7$ TeV using the ATLAS detector and determination of the strong coupling constant $\alpha_s(m_Z)$*, *Phys. Lett. B* **750** (2015) 427 [arXiv:1508.01579] [INSPIRE].

[7] ATLAS collaboration, *Determination of the strong coupling constant α_s from transverse energy-energy correlations in multijet events at $\sqrt{s} = 8$ TeV using the ATLAS detector*, *Eur. Phys. J. C* **77** (2017) 872 [arXiv:1707.02562] [INSPIRE].

[8] CMS collaboration, *Event shape variables measured using multijet final states in proton-proton collisions at $\sqrt{s} = 13$ TeV*, *JHEP* **12** (2018) 117 [arXiv:1811.00588] [INSPIRE].

[9] ATLAS collaboration, *Determination of the strong coupling constant from transverse energy-energy correlations in multijet events at $\sqrt{s} = 13$ TeV with the ATLAS detector*, *JHEP* **07** (2023) 085 [arXiv:2301.09351] [INSPIRE].

[10] D.E. Kaplan and M.D. Schwartz, *Constraining Light Colored Particles with Event Shapes*, *Phys. Rev. Lett.* **101** (2008) 022002 [arXiv:0804.2477] [INSPIRE].

[11] J. Llorente and B.P. Nachman, *Limits on new coloured fermions using precision jet data from the Large Hadron Collider*, *Nucl. Phys. B* **936** (2018) 106 [arXiv:1807.00894] [INSPIRE].

[12] T. Becher and M.D. Schwartz, *A precise determination of α_s from LEP thrust data using effective field theory*, *JHEP* **07** (2008) 034 [arXiv:0803.0342] [INSPIRE].

[13] R. Abbate et al., *Thrust at N^3LL with Power Corrections and a Precision Global Fit for $\alpha_s(mZ)$*, *Phys. Rev. D* **83** (2011) 074021 [arXiv:1006.3080] [INSPIRE].

[14] Y.-T. Chien and M.D. Schwartz, *Resummation of heavy jet mass and comparison to LEP data*, *JHEP* **08** (2010) 058 [arXiv:1005.1644] [INSPIRE].

[15] A.H. Hoang, D.W. Kolodrubetz, V. Mateu and I.W. Stewart, *C-parameter distribution at N^3LL' including power corrections*, *Phys. Rev. D* **91** (2015) 094017 [arXiv:1411.6633] [INSPIRE].

[16] C. Duhr, B. Mistlberger and G. Vita, *Four-Loop Rapidity Anomalous Dimension and Event Shapes to Fourth Logarithmic Order*, *Phys. Rev. Lett.* **129** (2022) 162001 [arXiv:2205.02242] [INSPIRE].

[17] A. Gehrmann-De Ridder, T. Gehrmann, E.W.N. Glover and G. Heinrich, *NNLO corrections to event shapes in e^+e^- annihilation*, *JHEP* **12** (2007) 094 [arXiv:0711.4711] [INSPIRE].

JHEP09(2024)072

[18] A. Gehrmann-De Ridder, T. Gehrmann, E.W.N. Glover and G. Heinrich, *Second-order QCD corrections to the thrust distribution*, *Phys. Rev. Lett.* **99** (2007) 132002 [arXiv:0707.1285] [INSPIRE].

[19] S. Weinzierl, *NNLO corrections to 3-jet observables in electron-positron annihilation*, *Phys. Rev. Lett.* **101** (2008) 162001 [arXiv:0807.3241] [INSPIRE].

[20] S. Weinzierl, *Event shapes and jet rates in electron-positron annihilation at NNLO*, *JHEP* **06** (2009) 041 [arXiv:0904.1077] [INSPIRE].

[21] V. Del Duca et al., *Three-Jet Production in Electron-Positron Collisions at Next-to-Next-to-Leading Order Accuracy*, *Phys. Rev. Lett.* **117** (2016) 152004 [arXiv:1603.08927] [INSPIRE].

[22] V. Del Duca et al., *Jet production in the CoLoRFulNNLO method: event shapes in electron-positron collisions*, *Phys. Rev. D* **94** (2016) 074019 [arXiv:1606.03453] [INSPIRE].

[23] B.R. Webber, *Estimation of power corrections to hadronic event shapes*, *Phys. Lett. B* **339** (1994) 148 [hep-ph/9408222] [INSPIRE].

[24] Y.L. Dokshitzer, G. Marchesini and B.R. Webber, *Dispersive approach to power behaved contributions in QCD hard processes*, *Nucl. Phys. B* **469** (1996) 93 [hep-ph/9512336] [INSPIRE].

[25] Y.L. Dokshitzer and B.R. Webber, *Calculation of power corrections to hadronic event shapes*, *Phys. Lett. B* **352** (1995) 451 [hep-ph/9504219] [INSPIRE].

[26] P. Nason and M.H. Seymour, *Infrared renormalons and power suppressed effects in e^+e^- jet events*, *Nucl. Phys. B* **454** (1995) 291 [hep-ph/9506317] [INSPIRE].

[27] A.V. Manohar and M.B. Wise, *Power suppressed corrections to hadronic event shapes*, *Phys. Lett. B* **344** (1995) 407 [hep-ph/9406392] [INSPIRE].

[28] E. Gardi and J. Rathsman, *Renormalon resummation and exponentiation of soft and collinear gluon radiation in the thrust distribution*, *Nucl. Phys. B* **609** (2001) 123 [hep-ph/0103217] [INSPIRE].

[29] Y.L. Dokshitzer, A. Lucenti, G. Marchesini and G.P. Salam, *On the universality of the Milan factor for 1/Q power corrections to jet shapes*, *JHEP* **05** (1998) 003 [hep-ph/9802381] [INSPIRE].

[30] Y.L. Dokshitzer, G. Marchesini and G.P. Salam, *Revisiting nonperturbative effects in the jet broadenings*, *Eur. Phys. J. direct* **1** (1999) 3 [hep-ph/9812487] [INSPIRE].

[31] S.T. Schindler, I.W. Stewart and Z. Sun, *Renormalons in the energy-energy correlator*, *JHEP* **10** (2023) 187 [arXiv:2305.19311] [INSPIRE].

[32] G. Bell et al., *Effects of renormalon scheme and perturbative scale choices on determinations of the strong coupling from e^+e^- event shapes*, *Phys. Rev. D* **109** (2024) 094008 [arXiv:2311.03990] [INSPIRE].

[33] G.P. Salam and D. Wicke, *Hadron masses and power corrections to event shapes*, *JHEP* **05** (2001) 061 [hep-ph/0102343] [INSPIRE].

[34] V. Mateu, I.W. Stewart and J. Thaler, *Power Corrections to Event Shapes with Mass-Dependent Operators*, *Phys. Rev. D* **87** (2013) 014025 [arXiv:1209.3781] [INSPIRE].

[35] G. Luisoni, P.F. Monni and G.P. Salam, *C-parameter hadronisation in the symmetric 3-jet limit and impact on α_s fits*, *Eur. Phys. J. C* **81** (2021) 158 [arXiv:2012.00622] [INSPIRE].

[36] F. Caola et al., *On linear power corrections in certain collider observables*, *JHEP* **01** (2022) 093 [arXiv:2108.08897] [INSPIRE].

JHEP09(2024)072

[37] J. Collins and J.-W. Qiu, *k_T factorization is violated in production of high-transverse-momentum particles in hadron-hadron collisions*, *Phys. Rev. D* **75** (2007) 114014 [arXiv:0705.2141] [INSPIRE].

[38] J. Collins, *2-soft-gluon exchange and factorization breaking*, arXiv:0708.4410 [INSPIRE].

[39] C.J. Bomhof, P.J. Mulders, W. Vogelsang and F. Yuan, *Single-Transverse Spin Asymmetry in Dijet Correlations at Hadron Colliders*, *Phys. Rev. D* **75** (2007) 074019 [hep-ph/0701277] [INSPIRE].

[40] T.C. Rogers and P.J. Mulders, *No Generalized TMD-Factorization in Hadro-Production of High Transverse Momentum Hadrons*, *Phys. Rev. D* **81** (2010) 094006 [arXiv:1001.2977] [INSPIRE].

[41] M.G.A. Buffing and P.J. Mulders, *Color entanglement for azimuthal asymmetries in the Drell-Yan process*, *Phys. Rev. Lett.* **112** (2014) 092002 [arXiv:1309.4681] [INSPIRE].

[42] J.R. Gaunt, *Glauber Gluons and Multiple Parton Interactions*, *JHEP* **07** (2014) 110 [arXiv:1405.2080] [INSPIRE].

[43] M. Zeng, *Drell-Yan process with jet vetoes: breaking of generalized factorization*, *JHEP* **10** (2015) 189 [arXiv:1507.01652] [INSPIRE].

[44] S. Catani, D. de Florian and G. Rodrigo, *Space-like (versus time-like) collinear limits in QCD: Is factorization violated?*, *JHEP* **07** (2012) 026 [arXiv:1112.4405] [INSPIRE].

[45] M.D. Schwartz, K. Yan and H.X. Zhu, *Collinear factorization violation and effective field theory*, *Phys. Rev. D* **96** (2017) 056005 [arXiv:1703.08572] [INSPIRE].

[46] J.R. Forshaw, A. Kyrieleis and M.H. Seymour, *Super-leading logarithms in non-global observables in QCD: Colour basis independent calculation*, *JHEP* **09** (2008) 128 [arXiv:0808.1269] [INSPIRE].

[47] J.R. Forshaw, A. Kyrieleis and M.H. Seymour, *Super-leading logarithms in non-global observables in QCD*, *JHEP* **08** (2006) 059 [hep-ph/0604094] [INSPIRE].

[48] R. Ángeles Martínez et al., *Soft gluon evolution and non-global logarithms*, *JHEP* **05** (2018) 044 [arXiv:1802.08531] [INSPIRE].

[49] R. Ángeles Martínez, J.R. Forshaw and M.H. Seymour, *Ordering multiple soft gluon emissions*, *Phys. Rev. Lett.* **116** (2016) 212003 [arXiv:1602.00623] [INSPIRE].

[50] J.R. Forshaw, M.H. Seymour and A. Siodmok, *On the Breaking of Collinear Factorization in QCD*, *JHEP* **11** (2012) 066 [arXiv:1206.6363] [INSPIRE].

[51] R. Ángeles-Martínez, J.R. Forshaw and M.H. Seymour, *Coulomb gluons and the ordering variable*, *JHEP* **12** (2015) 091 [arXiv:1510.07998] [INSPIRE].

[52] M.D. Schwartz, K. Yan and H.X. Zhu, *Factorization Violation and Scale Invariance*, *Phys. Rev. D* **97** (2018) 096017 [arXiv:1801.01138] [INSPIRE].

[53] I.Z. Rothstein and I.W. Stewart, *An Effective Field Theory for Forward Scattering and Factorization Violation*, *JHEP* **08** (2016) 025 [arXiv:1601.04695] [INSPIRE].

[54] J.R. Forshaw and J. Holguin, *Coulomb gluons will generally destroy coherence*, *JHEP* **12** (2021) 084 [*Erratum ibid.* **04** (2024) 097] [arXiv:2109.03665] [INSPIRE].

[55] L.J. Dixon, E. Herrmann, K. Yan and H.X. Zhu, *Soft gluon emission at two loops in full color*, *JHEP* **05** (2020) 135 [*Erratum ibid.* **06** (2024) 143] [arXiv:1912.09370] [INSPIRE].

[56] M. Alvarez et al., *NNLO QCD corrections to event shapes at the LHC*, *JHEP* **03** (2023) 129 [arXiv:2301.01086] [INSPIRE].

JHEP09(2024)072

[57] A. Banfi, G.P. Salam and G. Zanderighi, *Resummed event shapes at hadron-hadron colliders*, *JHEP* **08** (2004) 062 [hep-ph/0407287] [INSPIRE].

[58] A. Banfi, G.P. Salam and G. Zanderighi, *Phenomenology of event shapes at hadron colliders*, *JHEP* **06** (2010) 038 [arXiv:1001.4082] [INSPIRE].

[59] I.W. Stewart, F.J. Tackmann and W.J. Waalewijn, *The Beam Thrust Cross Section for Drell-Yan at NNLL Order*, *Phys. Rev. Lett.* **106** (2011) 032001 [arXiv:1005.4060] [INSPIRE].

[60] T. Becher, X. Garcia i Tormo and J. Piclum, *Next-to-next-to-leading logarithmic resummation for transverse thrust*, *Phys. Rev. D* **93** (2016) 054038 [*Erratum ibid.* **93** (2016) 079905] [arXiv:1512.00022] [INSPIRE].

[61] T. Becher and X. Garcia i Tormo, *Factorization and resummation for transverse thrust*, *JHEP* **06** (2015) 071 [arXiv:1502.04136] [INSPIRE].

[62] T.T. Jouttenus, I.W. Stewart, F.J. Tackmann and W.J. Waalewijn, *Jet mass spectra in Higgs boson plus one jet at next-to-next-to-leading logarithmic order*, *Phys. Rev. D* **88** (2013) 054031 [arXiv:1302.0846] [INSPIRE].

[63] S. Alioli et al., *N3LL resummation of one-jettiness for Z-boson plus jet production at hadron colliders*, *Phys. Rev. D* **109** (2024) 094009 [arXiv:2312.06496] [INSPIRE].

[64] A.J. Gao, H.T. Li, I. Moult and H.X. Zhu, *Precision QCD Event Shapes at Hadron Colliders: The Transverse Energy-Energy Correlator in the Back-to-Back Limit*, *Phys. Rev. Lett.* **123** (2019) 062001 [arXiv:1901.04497] [INSPIRE].

[65] A. Ali, F. Barreiro, J. Llorente and W. Wang, *Transverse Energy-Energy Correlations in Next-to-Leading Order in α_s at the LHC*, *Phys. Rev. D* **86** (2012) 114017 [arXiv:1205.1689] [INSPIRE].

[66] H.T. Li, Y. Makris and I. Vitev, *Energy-energy correlators in Deep Inelastic Scattering*, *Phys. Rev. D* **103** (2021) 094005 [arXiv:2102.05669] [INSPIRE].

[67] H.T. Li, I. Vitev and Y.J. Zhu, *Transverse-Energy-Energy Correlations in Deep Inelastic Scattering*, *JHEP* **11** (2020) 051 [arXiv:2006.02437] [INSPIRE].

[68] Z.-B. Kang, J. Penttala, F. Zhao and Y. Zhou, *Transverse energy-energy correlators in the color-glass condensate at the electron-ion collider*, *Phys. Rev. D* **109** (2024) 094012 [arXiv:2311.17142] [INSPIRE].

[69] H. Cao, H.T. Li and Z. Mi, *Bjorken × weighted energy-energy correlators from the target fragmentation region to the current fragmentation region*, *Phys. Rev. D* **109** (2024) 096004 [arXiv:2312.07655] [INSPIRE].

[70] L.J. Dixon et al., *Analytical Computation of Energy-Energy Correlation at Next-to-Leading Order in QCD*, *Phys. Rev. Lett.* **120** (2018) 102001 [arXiv:1801.03219] [INSPIRE].

[71] M.-X. Luo, V. Shtabovenko, T.-Z. Yang and H.X. Zhu, *Analytic Next-To-Leading Order Calculation of Energy-Energy Correlation in Gluon-Initiated Higgs Decays*, *JHEP* **06** (2019) 037 [arXiv:1903.07277] [INSPIRE].

[72] J. Gao, V. Shtabovenko and T.-Z. Yang, *Energy-energy correlation in hadronic Higgs decays: analytic results and phenomenology at NLO*, *JHEP* **02** (2021) 210 [arXiv:2012.14188] [INSPIRE].

[73] A.V. Belitsky et al., *From correlation functions to event shapes*, *Nucl. Phys. B* **884** (2014) 305 [arXiv:1309.0769] [INSPIRE].

JHEP09(2024)072

[74] A.V. Belitsky et al., *Event shapes in $\mathcal{N} = 4$ super-Yang-Mills theory*, *Nucl. Phys. B* **884** (2014) 206 [arXiv:1309.1424] [INSPIRE].

[75] A.V. Belitsky et al., *Energy-Energy Correlations in $N = 4$ Supersymmetric Yang-Mills Theory*, *Phys. Rev. Lett.* **112** (2014) 071601 [arXiv:1311.6800] [INSPIRE].

[76] J.M. Henn, E. Sokatchev, K. Yan and A. Zhiboedov, *Energy-energy correlation in $N = 4$ super Yang-Mills theory at next-to-next-to-leading order*, *Phys. Rev. D* **100** (2019) 036010 [arXiv:1903.05314] [INSPIRE].

[77] I. Moult and H.X. Zhu, *Simplicity from Recoil: The Three-Loop Soft Function and Factorization for the Energy-Energy Correlation*, *JHEP* **08** (2018) 160 [arXiv:1801.02627] [INSPIRE].

[78] M.A. Ebert, B. Mistlberger and G. Vita, *The Energy-Energy Correlation in the back-to-back limit at N^3LO and N^3LL'*, *JHEP* **08** (2021) 022 [arXiv:2012.07859] [INSPIRE].

[79] L.J. Dixon, I. Moult and H.X. Zhu, *Collinear limit of the energy-energy correlator*, *Phys. Rev. D* **100** (2019) 014009 [arXiv:1905.01310] [INSPIRE].

[80] M. Kologlu, P. Kravchuk, D. Simmons-Duffin and A. Zhiboedov, *The light-ray OPE and conformal colliders*, *JHEP* **01** (2021) 128 [arXiv:1905.01311] [INSPIRE].

[81] G.P. Korchemsky, *Energy correlations in the end-point region*, *JHEP* **01** (2020) 008 [arXiv:1905.01444] [INSPIRE].

[82] H. Chen, I. Moult, X.Y. Zhang and H.X. Zhu, *Rethinking jets with energy correlators: Tracks, resummation, and analytic continuation*, *Phys. Rev. D* **102** (2020) 054012 [arXiv:2004.11381] [INSPIRE].

[83] H. Chen, *QCD factorization from light-ray OPE*, *JHEP* **01** (2024) 035 [arXiv:2311.00350] [INSPIRE].

[84] Z. Tulipánt, A. Kardos and G. Somogyi, *Energy-energy correlation in electron-positron annihilation at NNLL + NNLO accuracy*, *Eur. Phys. J. C* **77** (2017) 749 [arXiv:1708.04093] [INSPIRE].

[85] H. Chen et al., *Three point energy correlators in the collinear limit: symmetries, dualities and analytic results*, *JHEP* **08** (2020) 028 [arXiv:1912.11050] [INSPIRE].

[86] K. Yan and X. Zhang, *Three-Point Energy Correlator in $N = 4$ Supersymmetric Yang-Mills Theory*, *Phys. Rev. Lett.* **129** (2022) 021602 [arXiv:2203.04349] [INSPIRE].

[87] T.-Z. Yang and X. Zhang, *Analytic Computation of three-point energy correlator in QCD*, *JHEP* **09** (2022) 006 [arXiv:2208.01051] [INSPIRE].

[88] P.T. Komiske, I. Moult, J. Thaler and H.X. Zhu, *Analyzing N-Point Energy Correlators inside Jets with CMS Open Data*, *Phys. Rev. Lett.* **130** (2023) 051901 [arXiv:2201.07800] [INSPIRE].

[89] J. Holguin, I. Moult, A. Pathak and M. Procura, *New paradigm for precision top physics: Weighing the top with energy correlators*, *Phys. Rev. D* **107** (2023) 114002 [arXiv:2201.08393] [INSPIRE].

[90] X. Liu and H.X. Zhu, *Nucleon Energy Correlators*, *Phys. Rev. Lett.* **130** (2023) 091901 [arXiv:2209.02080] [INSPIRE].

[91] H.-Y. Liu et al., *Nucleon Energy Correlators for the Color Glass Condensate*, *Phys. Rev. Lett.* **130** (2023) 181901 [arXiv:2301.01788] [INSPIRE].

[92] H. Cao, X. Liu and H.X. Zhu, *Toward precision measurements of nucleon energy correlators in lepton-nucleon collisions*, *Phys. Rev. D* **107** (2023) 114008 [arXiv:2303.01530] [INSPIRE].

JHEP09(2024)072

[93] K. Devereaux et al., *Imaging Cold Nuclear Matter with Energy Correlators*, arXiv:2303.08143 [INSPIRE].

[94] C. Andres et al., *Resolving the Scales of the Quark-Gluon Plasma with Energy Correlators*, *Phys. Rev. Lett.* **130** (2023) 262301 [arXiv:2209.11236] [INSPIRE].

[95] C. Andres et al., *A coherent view of the quark-gluon plasma from energy correlators*, *JHEP* **09** (2023) 088 [arXiv:2303.03413] [INSPIRE].

[96] E. Craft, K. Lee, B. Meçaj and I. Moult, *Beautiful and Charming Energy Correlators*, arXiv:2210.09311 [INSPIRE].

[97] K. Lee, B. Meçaj and I. Moult, *Conformal Colliders Meet the LHC*, arXiv:2205.03414 [INSPIRE].

[98] J. Barata, J.G. Milhano and A.V. Sadofyev, *Picturing QCD jets in anisotropic matter: from jet shapes to energy energy correlators*, *Eur. Phys. J. C* **84** (2024) 174 [arXiv:2308.01294] [INSPIRE].

[99] J. Barata, P. Caucal, A. Soto-Ontoso and R. Szafron, *Advancing the understanding of energy-energy correlators in heavy-ion collisions*, arXiv:2312.12527 [INSPIRE].

[100] C.W. Bauer, S. Fleming and M.E. Luke, *Summing Sudakov logarithms in $B \to X_s\gamma$in effective field theory*, *Phys. Rev. D* **63** (2000) 014006 [hep-ph/0005275] [INSPIRE].

[101] C.W. Bauer, S. Fleming, D. Pirjol and I.W. Stewart, *An effective field theory for collinear and soft gluons: Heavy to light decays*, *Phys. Rev. D* **63** (2001) 114020 [hep-ph/0011336] [INSPIRE].

[102] C.W. Bauer and I.W. Stewart, *Invariant operators in collinear effective theory*, *Phys. Lett. B* **516** (2001) 134 [hep-ph/0107001] [INSPIRE].

[103] C.W. Bauer, D. Pirjol and I.W. Stewart, *Soft collinear factorization in effective field theory*, *Phys. Rev. D* **65** (2002) 054022 [hep-ph/0109045] [INSPIRE].

[104] O. Almelid, C. Duhr and E. Gardi, *Three-loop corrections to the soft anomalous dimension in multileg scattering*, *Phys. Rev. Lett.* **117** (2016) 172002 [arXiv:1507.00047] [INSPIRE].

[105] O. Almelid et al., *Bootstrapping the QCD soft anomalous dimension*, *JHEP* **09** (2017) 073 [arXiv:1706.10162] [INSPIRE].

[106] Y. Li and H.X. Zhu, *Bootstrapping Rapidity Anomalous Dimensions for Transverse-Momentum Resummation*, *Phys. Rev. Lett.* **118** (2017) 022004 [arXiv:1604.01404] [INSPIRE].

[107] S. Moch et al., *On quartic colour factors in splitting functions and the gluon cusp anomalous dimension*, *Phys. Lett. B* **782** (2018) 627 [arXiv:1805.09638] [INSPIRE].

[108] S. Moch et al., *Four-Loop Non-Singlet Splitting Functions in the Planar Limit and Beyond*, *JHEP* **10** (2017) 041 [arXiv:1707.08315] [INSPIRE].

[109] J. Davies et al., *Large-nf contributions to the four-loop splitting functions in QCD*, *Nucl. Phys. B* **915** (2017) 335 [arXiv:1610.07477] [INSPIRE].

[110] J.M. Henn, G.P. Korchemsky and B. Mistlberger, *The full four-loop cusp anomalous dimension in $\mathcal{N} = 4$ super Yang-Mills and QCD*, *JHEP* **04** (2020) 018 [arXiv:1911.10174] [INSPIRE].

[111] T. Gehrmann, T. Lübbert and L.L. Yang, *Transverse parton distribution functions at next-to-next-to-leading order: the quark-to-quark case*, *Phys. Rev. Lett.* **109** (2012) 242003 [arXiv:1209.0682] [INSPIRE].

[112] T. Gehrmann, T. Luebbert and L.L. Yang, *Calculation of the transverse parton distribution functions at next-to-next-to-leading order*, *JHEP* **06** (2014) 155 [arXiv:1403.6451] [INSPIRE].

JHEP09(2024)072

[113] M.G. Echevarria, I. Scimemi and A. Vladimirov, *Unpolarized Transverse Momentum Dependent Parton Distribution and Fragmentation Functions at next-to-next-to-leading order*, *JHEP* **09** (2016) 004 [arXiv:1604.07869] [INSPIRE].

[114] T. Lübbert, J. Oredsson and M. Stahlhofen, *Rapidity renormalized TMD soft and beam functions at two loops*, *JHEP* **03** (2016) 168 [arXiv:1602.01829] [INSPIRE].

[115] M.-X. Luo et al., *Transverse Parton Distribution and Fragmentation Functions at NNLO: the Quark Case*, *JHEP* **10** (2019) 083 [arXiv:1908.03831] [INSPIRE].

[116] M.-X. Luo, T.-Z. Yang, H.X. Zhu and Y.J. Zhu, *Transverse Parton Distribution and Fragmentation Functions at NNLO: the Gluon Case*, *JHEP* **01** (2020) 040 [arXiv:1909.13820] [INSPIRE].

[117] C. Anastasiou, E.W.N. Glover, C. Oleari and M.E. Tejeda-Yeomans, *Two-loop QCD corrections to the scattering of massless distinct quarks*, *Nucl. Phys. B* **601** (2001) 318 [hep-ph/0010212] [INSPIRE].

[118] C. Anastasiou, E.W.N. Glover, C. Oleari and M.E. Tejeda-Yeomans, *Two loop QCD corrections to massless identical quark scattering*, *Nucl. Phys. B* **601** (2001) 341 [hep-ph/0011094] [INSPIRE].

[119] E.W.N. Glover, C. Oleari and M.E. Tejeda-Yeomans, *Two loop QCD corrections to gluon-gluon scattering*, *Nucl. Phys. B* **605** (2001) 467 [hep-ph/0102201] [INSPIRE].

[120] Z. Bern, A. De Freitas and L.J. Dixon, *Two loop helicity amplitudes for gluon-gluon scattering in QCD and supersymmetric Yang-Mills theory*, *JHEP* **03** (2002) 018 [hep-ph/0201161] [INSPIRE].

[121] Z. Bern, A. De Freitas and L.J. Dixon, *Two loop helicity amplitudes for quark gluon scattering in QCD and gluino gluon scattering in supersymmetric Yang-Mills theory*, *JHEP* **06** (2003) 028 [*Erratum ibid.* **04** (2014) 112] [hep-ph/0304168] [INSPIRE].

[122] E.W.N. Glover and M.E. Tejeda-Yeomans, *Two loop QCD helicity amplitudes for massless quark massless gauge boson scattering*, *JHEP* **06** (2003) 033 [hep-ph/0304169] [INSPIRE].

[123] E.W.N. Glover, *Two loop QCD helicity amplitudes for massless quark quark scattering*, *JHEP* **04** (2004) 021 [hep-ph/0401119] [INSPIRE].

[124] A. De Freitas and Z. Bern, *Two-loop helicity amplitudes for quark-quark scattering in QCD and gluino-gluino scattering in supersymmetric Yang-Mills theory*, *JHEP* **09** (2004) 039 [hep-ph/0409007] [INSPIRE].

[125] M. Czakon, A. Mitov and R. Poncelet, *Next-to-Next-to-Leading Order Study of Three-Jet Production at the LHC*, *Phys. Rev. Lett.* **127** (2021) 152001 [*Erratum ibid.* **129** (2022) 119901] [arXiv:2106.05331] [INSPIRE].

[126] S. Abreu et al., *All Two-Loop Feynman Integrals for Five-Point One-Mass Scattering*, *Phys. Rev. Lett.* **132** (2024) 141601 [arXiv:2306.15431] [INSPIRE].

[127] D. Chicherin, V. Sotnikov and S. Zoia, *Pentagon functions for one-mass planar scattering amplitudes*, *JHEP* **01** (2022) 096 [arXiv:2110.10111] [INSPIRE].

[128] D. Chicherin and V. Sotnikov, *Pentagon Functions for Scattering of Five Massless Particles*, *JHEP* **12** (2020) 167 [arXiv:2009.07803] [INSPIRE].

[129] S. Badger et al., *Analytic form of the full two-loop five-gluon all-plus helicity amplitude*, *Phys. Rev. Lett.* **123** (2019) 071601 [arXiv:1905.03733] [INSPIRE].

JHEP09(2024)072

[130] D. Chicherin et al., *All Master Integrals for Three-Jet Production at Next-to-Next-to-Leading Order*, *Phys. Rev. Lett.* **123** (2019) 041603 [arXiv:1812.11160] [INSPIRE].

[131] D. Chicherin et al., *Analytic result for the nonplanar hexa-box integrals*, *JHEP* **03** (2019) 042 [arXiv:1809.06240] [INSPIRE].

[132] D. Chicherin et al., *Analytic result for a two-loop five-particle amplitude*, *Phys. Rev. Lett.* **122** (2019) 121602 [arXiv:1812.11057] [INSPIRE].

[133] S. Abreu et al., *The two-loop five-point amplitude in $\mathcal{N} = 4$ super-Yang-Mills theory*, *Phys. Rev. Lett.* **122** (2019) 121603 [arXiv:1812.08941] [INSPIRE].

[134] T. Gehrmann, J.M. Henn and N.A. Lo Presti, *Analytic form of the two-loop planar five-gluon all-plus-helicity amplitude in QCD*, *Phys. Rev. Lett.* **116** (2016) 062001 [*Erratum ibid.* **116** (2016) 189903] [arXiv:1511.05409] [INSPIRE].

[135] S. Abreu et al., *Planar Two-Loop Five-Parton Amplitudes from Numerical Unitarity*, *JHEP* **11** (2018) 116 [arXiv:1809.09067] [INSPIRE].

[136] S. Abreu et al., *Planar Two-Loop Five-Gluon Amplitudes from Numerical Unitarity*, *Phys. Rev. D* **97** (2018) 116014 [arXiv:1712.03946] [INSPIRE].

[137] S. Abreu et al., *Analytic Form of Planar Two-Loop Five-Gluon Scattering Amplitudes in QCD*, *Phys. Rev. Lett.* **122** (2019) 082002 [arXiv:1812.04586] [INSPIRE].

[138] M.-X. Luo, T.-Z. Yang, H.X. Zhu and Y.J. Zhu, *Quark Transverse Parton Distribution at the Next-to-Next-to-Next-to-Leading Order*, *Phys. Rev. Lett.* **124** (2020) 092001 [arXiv:1912.05778] [INSPIRE].

[139] M.-X. Luo, T.-Z. Yang, H.X. Zhu and Y.J. Zhu, *Unpolarized quark and gluon TMD PDFs and FFs at N^3LO*, *JHEP* **06** (2021) 115 [arXiv:2012.03256] [INSPIRE].

[140] M.A. Ebert, B. Mistlberger and G. Vita, *TMD fragmentation functions at N^3LO*, *JHEP* **07** (2021) 121 [arXiv:2012.07853] [INSPIRE].

[141] M.A. Ebert, B. Mistlberger and G. Vita, *Transverse momentum dependent PDFs at N^3LO*, *JHEP* **09** (2020) 146 [arXiv:2006.05329] [INSPIRE].

[142] I. Moult, H.X. Zhu and Y.J. Zhu, *The four loop QCD rapidity anomalous dimension*, *JHEP* **08** (2022) 280 [arXiv:2205.02249] [INSPIRE].

[143] P. Bargiela, F. Caola, A. von Manteuffel and L. Tancredi, *Three-loop helicity amplitudes for diphoton production in gluon fusion*, *JHEP* **02** (2022) 153 [arXiv:2111.13595] [INSPIRE].

[144] F. Caola et al., *Three-Loop Gluon Scattering in QCD and the Gluon Regge Trajectory*, *Phys. Rev. Lett.* **128** (2022) 212001 [arXiv:2112.11097] [INSPIRE].

[145] F. Caola et al., *Three-loop helicity amplitudes for four-quark scattering in massless QCD*, *JHEP* **10** (2021) 206 [arXiv:2108.00055] [INSPIRE].

[146] F. Caola, A. Von Manteuffel and L. Tancredi, *Diphoton Amplitudes in Three-Loop Quantum Chromodynamics*, *Phys. Rev. Lett.* **126** (2021) 112004 [arXiv:2011.13946] [INSPIRE].

[147] J.C. Collins and D.E. Soper, *Back-To-Back Jets in QCD*, *Nucl. Phys. B* **193** (1981) 381 [*Erratum ibid.* **213** (1983) 545] [INSPIRE].

[148] J.C. Collins and D.E. Soper, *Back-To-Back Jets: Fourier Transform from B to K-Transverse*, *Nucl. Phys. B* **197** (1982) 446 [INSPIRE].

[149] J.C. Collins and G.F. Sterman, *Soft Partons in QCD*, *Nucl. Phys. B* **185** (1981) 172 [INSPIRE].

JHEP09(2024)072

[150] J.C. Collins, D.E. Soper and G.F. Sterman, *Transverse Momentum Distribution in Drell-Yan Pair and W and Z Boson Production*, *Nucl. Phys. B* **250** (1985) 199 [INSPIRE].

[151] J.C. Collins, D.E. Soper and G.F. Sterman, *Factorization for Short Distance Hadron-Hadron Scattering*, *Nucl. Phys. B* **261** (1985) 104 [INSPIRE].

[152] J.C. Collins, D.E. Soper and G.F. Sterman, *Soft Gluons and Factorization*, *Nucl. Phys. B* **308** (1988) 833 [INSPIRE].

[153] J.C. Collins, D.E. Soper and G.F. Sterman, *Factorization of Hard Processes in QCD*, *Adv. Ser. Direct. High Energy Phys.* **5** (1989) 1 [hep-ph/0409313] [INSPIRE].

[154] C.L. Basham, L.S. Brown, S.D. Ellis and S.T. Love, *Energy Correlations in Perturbative Quantum Chromodynamics: A Conjecture for All Orders*, *Phys. Lett. B* **85** (1979) 297 [INSPIRE].

[155] C.L. Basham, L.S. Brown, S.D. Ellis and S.T. Love, *Energy Correlations in electron-Positron Annihilation in Quantum Chromodynamics: Asymptotically Free Perturbation Theory*, *Phys. Rev. D* **19** (1979) 2018 [INSPIRE].

[156] C.L. Basham, L.S. Brown, S.D. Ellis and S.T. Love, *Energy Correlations in electron-Positron Annihilation: Testing QCD*, *Phys. Rev. Lett.* **41** (1978) 1585 [INSPIRE].

[157] C.L. Basham, L.S. Brown, S.D. Ellis and S.T. Love, *Electron-Positron Annihilation Energy Pattern in Quantum Chromodynamics: Asymptotically Free Perturbation Theory*, *Phys. Rev. D* **17** (1978) 2298 [INSPIRE].

[158] A. Ali, E. Pietarinen and W.J. Stirling, *Transverse Energy-energy Correlations: A Test of Perturbative QCD for the Proton-Anti-proton Collider*, *Phys. Lett. B* **141** (1984) 447 [INSPIRE].

[159] J. Kalinowski, K. Konishi, P.N. Scharbach and T.R. Taylor, *Resolving qcd jets beyond leading order: quark decay probabilities*, *Nucl. Phys. B* **181** (1981) 253 [INSPIRE].

[160] K. Konishi, A. Ukawa and G. Veneziano, *Jet Calculus: A Simple Algorithm for Resolving QCD Jets*, *Nucl. Phys. B* **157** (1979) 45 [INSPIRE].

[161] D.G. Richards, W.J. Stirling and S.D. Ellis, *Second Order Corrections to the Energy-energy Correlation Function in Quantum Chromodynamics*, *Phys. Lett. B* **119** (1982) 193 [INSPIRE].

[162] H.B. Hartanto, S. Badger, C. Brønnum-Hansen and T. Peraro, *A numerical evaluation of planar two-loop helicity amplitudes for a W-boson plus four partons*, *JHEP* **09** (2019) 119 [arXiv:1906.11862] [INSPIRE].

[163] A. Banfi, G. Marchesini and G. Smye, *Azimuthal correlation in DIS*, *JHEP* **04** (2002) 024 [hep-ph/0203150] [INSPIRE].

[164] M.G.A. Buffing, Z.-B. Kang, K. Lee and X. Liu, *A transverse momentum dependent framework for back-to-back photon+jet production*, arXiv:1812.07549 [INSPIRE].

[165] Y.-T. Chien, D.Y. Shao and B. Wu, *Resummation of Boson-Jet Correlation at Hadron Colliders*, *JHEP* **11** (2019) 025 [arXiv:1905.01335] [INSPIRE].

[166] Y.-T. Chien et al., *Precision boson-jet azimuthal decorrelation at hadron colliders*, *JHEP* **02** (2023) 256 [arXiv:2205.05104] [INSPIRE].

[167] Y.-T. Chien et al., *Recoil-free azimuthal angle for precision boson-jet correlation*, *Phys. Lett. B* **815** (2021) 136124 [arXiv:2005.12279] [INSPIRE].

[168] I.W. Stewart, F.J. Tackmann and W.J. Waalewijn, *Factorization at the LHC: From PDFs to Initial State Jets*, *Phys. Rev. D* **81** (2010) 094035 [arXiv:0910.0467] [INSPIRE].

JHEP09(2024)072

[169] H. Georgi and H.D. Politzer, *Quark Decay Functions and Heavy Hadron Production in QCD*, *Nucl. Phys. B* **136** (1978) 445 [INSPIRE].

[170] R.K. Ellis et al., *Perturbation Theory and the Parton Model in QCD*, *Nucl. Phys. B* **152** (1979) 285 [INSPIRE].

[171] J.C. Collins and D.E. Soper, *Parton Distribution and Decay Functions*, *Nucl. Phys. B* **194** (1982) 445 [INSPIRE].

[172] J. Collins, *Foundations of Perturbative QCD*, Cambridge University Press (2023) [DOI:10.1017/9781009401845] [INSPIRE].

[173] I. Moult, I.W. Stewart, F.J. Tackmann and W.J. Waalewijn, *Employing Helicity Amplitudes for Resummation*, *Phys. Rev. D* **93** (2016) 094003 [arXiv:1508.02397] [INSPIRE].

[174] Z. Kunszt, A. Signer and Z. Trócsányi, *One loop helicity amplitudes for all* $2 \to 2$ *processes in QCD and* $N = 1$ *supersymmetric Yang-Mills theory*, *Nucl. Phys. B* **411** (1994) 397 [hep-ph/9305239] [INSPIRE].

[175] R. Kelley and M.D. Schwartz, *1-loop matching and NNLL resummation for all partonic 2 to 2 processes in QCD*, *Phys. Rev. D* **83** (2011) 045022 [arXiv:1008.2759] [INSPIRE].

[176] A. Broggio, A. Ferroglia, B.D. Pecjak and Z. Zhang, *NNLO hard functions in massless QCD*, *JHEP* **12** (2014) 005 [arXiv:1409.5294] [INSPIRE].

[177] S. Catani and M.H. Seymour, *A general algorithm for calculating jet cross-sections in NLO QCD*, *Nucl. Phys. B* **485** (1997) 291 [hep-ph/9605323] [INSPIRE].

[178] I.W. Stewart, F.J. Tackmann and W.J. Waalewijn, *The Quark Beam Function at NNLL*, *JHEP* **09** (2010) 005 [arXiv:1002.2213] [INSPIRE].

[179] S. Alioli, C.W. Bauer, S. Guns and F.J. Tackmann, *Underlying event sensitive observables in Drell-Yan production using GENEVA*, *Eur. Phys. J. C* **76** (2016) 614 [arXiv:1605.07192] [INSPIRE].

[180] M. Cacciari, G.P. Salam and S. Sapeta, *On the characterisation of the underlying event*, *JHEP* **04** (2010) 065 [arXiv:0912.4926] [INSPIRE].

[181] T. Sjostrand, S. Mrenna and P.Z. Skands, *PYTHIA 6.4 Physics and Manual*, *JHEP* **05** (2006) 026 [hep-ph/0603175] [INSPIRE].

[182] T. Sjostrand, S. Mrenna and P.Z. Skands, *A Brief Introduction to PYTHIA 8.1*, *Comput. Phys. Commun.* **178** (2008) 852 [arXiv:0710.3820] [INSPIRE].

[183] I.W. Stewart, F.J. Tackmann and W.J. Waalewijn, *Dissecting Soft Radiation with Factorization*, *Phys. Rev. Lett.* **114** (2015) 092001 [arXiv:1405.6722] [INSPIRE].

[184] T. Gehrmann et al., *Planar three-loop QCD helicity amplitudes for V+jet production at hadron colliders*, *Phys. Lett. B* **848** (2024) 138369 [arXiv:2307.15405] [INSPIRE].

[185] J.M. Henn, J. Lim and W.J. Torres Bobadilla, *First look at the evaluation of three-loop non-planar Feynman diagrams for Higgs plus jet production*, *JHEP* **05** (2023) 026 [arXiv:2302.12776] [INSPIRE].

[186] G. Bell, R. Rahn and J. Talbert, *Two-loop anomalous dimensions of generic dijet soft functions*, *Nucl. Phys. B* **936** (2018) 520 [arXiv:1805.12414] [INSPIRE].

[187] G. Bell, R. Rahn and J. Talbert, *Generic dijet soft functions at two-loop order: correlated emissions*, *JHEP* **07** (2019) 101 [arXiv:1812.08690] [INSPIRE].

JHEP09(2024)072

[188] G. Bell, B. Dehnadi, T. Mohrmann and R. Rahn, *Automated Calculation of N-jet Soft Functions*, *PoS* **LL2018** (2018) 044 [arXiv:1808.07427] [INSPIRE].

[189] G. Bell, B. Dehnadi, T. Mohrmann and R. Rahn, *The NNLO soft function for N-jettiness in hadronic collisions*, *JHEP* **07** (2024) 077 [arXiv:2312.11626] [INSPIRE].

[190] S. Jin and X. Liu, *Two-loop N-jettiness soft function for $pp \to 2j$ production*, *Phys. Rev. D* **99** (2019) 114017 [arXiv:1901.10935] [INSPIRE].

[191] L.J. Dixon, *The Principle of Maximal Transcendentality and the Four-Loop Collinear Anomalous Dimension*, *JHEP* **01** (2018) 075 [arXiv:1712.07274] [INSPIRE].

[192] Y. Li, A. von Manteuffel, R.M. Schabinger and H.X. Zhu, *N^3LO Higgs boson and Drell-Yan production at threshold: The one-loop two-emission contribution*, *Phys. Rev. D* **90** (2014) 053006 [arXiv:1404.5839] [INSPIRE].

[193] A. Vladimirov, *Structure of rapidity divergences in multi-parton scattering soft factors*, *JHEP* **04** (2018) 045 [arXiv:1707.07606] [INSPIRE].

[194] A.A. Vladimirov, *Correspondence between Soft and Rapidity Anomalous Dimensions*, *Phys. Rev. Lett.* **118** (2017) 062001 [arXiv:1610.05791] [INSPIRE].

[195] Y. Li, D. Neill and H.X. Zhu, *An exponential regulator for rapidity divergences*, *Nucl. Phys. B* **960** (2020) 115193 [arXiv:1604.00392] [INSPIRE].

[196] N. Kidonakis, G. Oderda and G.F. Sterman, *Threshold resummation for dijet cross-sections*, *Nucl. Phys. B* **525** (1998) 299 [hep-ph/9801268] [INSPIRE].

[197] N. Kidonakis, G. Oderda and G.F. Sterman, *Evolution of color exchange in QCD hard scattering*, *Nucl. Phys. B* **531** (1998) 365 [hep-ph/9803241] [INSPIRE].

[198] S.M. Aybat, L.J. Dixon and G.F. Sterman, *The Two-loop soft anomalous dimension matrix and resummation at next-to-next-to leading pole*, *Phys. Rev. D* **74** (2006) 074004 [hep-ph/0607309] [INSPIRE].

[199] S.M. Aybat, L.J. Dixon and G.F. Sterman, *The Two-loop anomalous dimension matrix for soft gluon exchange*, *Phys. Rev. Lett.* **97** (2006) 072001 [hep-ph/0606254] [INSPIRE].

[200] G.P. Korchemsky and A.V. Radyushkin, *Renormalization of the Wilson Loops Beyond the Leading Order*, *Nucl. Phys. B* **283** (1987) 342 [INSPIRE].

[201] Y. Li, A. von Manteuffel, R.M. Schabinger and H.X. Zhu, *Soft-virtual corrections to Higgs production at N^3LO*, *Phys. Rev. D* **91** (2015) 036008 [arXiv:1412.2771] [INSPIRE].

[202] J.-Y. Chiu, A. Jain, D. Neill and I.Z. Rothstein, *The Rapidity Renormalization Group*, *Phys. Rev. Lett.* **108** (2012) 151601 [arXiv:1104.0881] [INSPIRE].

[203] J.-Y. Chiu, A. Jain, D. Neill and I.Z. Rothstein, *A Formalism for the Systematic Treatment of Rapidity Logarithms in Quantum Field Theory*, *JHEP* **05** (2012) 084 [arXiv:1202.0814] [INSPIRE].

[204] J.G.M. Gatheral, *Exponentiation of Eikonal Cross-sections in Nonabelian Gauge Theories*, *Phys. Lett. B* **133** (1983) 90 [INSPIRE].

[205] J. Frenkel and J.C. Taylor, *Nonabelian eikonal exponentiation*, *Nucl. Phys. B* **246** (1984) 231 [INSPIRE].

[206] J.C. Collins and A. Metz, *Universality of soft and collinear factors in hard-scattering factorization*, *Phys. Rev. Lett.* **93** (2004) 252001 [hep-ph/0408249] [INSPIRE].

JHEP09(2024)072

[207] S. Catani and M. Grazzini, *Infrared factorization of tree level QCD amplitudes at the next-to-next-to-leading order and beyond*, *Nucl. Phys. B* **570** (2000) 287 [hep-ph/9908523] [INSPIRE].

[208] S. Catani and M. Grazzini, *The soft gluon current at one loop order*, *Nucl. Phys. B* **591** (2000) 435 [hep-ph/0007142] [INSPIRE].

[209] G. Falcioni, E. Gardi and C. Milloy, *Relating amplitude and PDF factorisation through Wilson-line geometries*, *JHEP* **11** (2019) 100 [arXiv:1909.00697] [INSPIRE].

[210] L.J. Dixon and I. Esterlis, *All orders results for self-crossing Wilson loops mimicking double parton scattering*, *JHEP* **07** (2016) 116 [*Erratum ibid.* **08** (2016) 131] [arXiv:1602.02107] [INSPIRE].

[211] L.J. Dixon, *Matter Dependence of the Three-Loop Soft Anomalous Dimension Matrix*, *Phys. Rev. D* **79** (2009) 091501 [arXiv:0901.3414] [INSPIRE].

[212] L.J. Dixon, L. Magnea and G.F. Sterman, *Universal structure of subleading infrared poles in gauge theory amplitudes*, *JHEP* **08** (2008) 022 [arXiv:0805.3515] [INSPIRE].

[213] E. Gardi and L. Magnea, *Infrared singularities in QCD amplitudes*, *Nuovo Cim. C* **32N5-6** (2009) 137 [arXiv:0908.3273] [INSPIRE].

[214] E. Gardi and L. Magnea, *Factorization constraints for soft anomalous dimensions in QCD scattering amplitudes*, *JHEP* **03** (2009) 079 [arXiv:0901.1091] [INSPIRE].

[215] L.J. Dixon, E. Gardi and L. Magnea, *On soft singularities at three loops and beyond*, *JHEP* **02** (2010) 081 [arXiv:0910.3653] [INSPIRE].

[216] T. Becher and M. Neubert, *Infrared singularities of scattering amplitudes in perturbative QCD*, *Phys. Rev. Lett.* **102** (2009) 162001 [*Erratum ibid.* **111** (2013) 199905] [arXiv:0901.0722] [INSPIRE].

[217] T. Becher and M. Neubert, *On the Structure of Infrared Singularities of Gauge-Theory Amplitudes*, *JHEP* **06** (2009) 081 [*Erratum ibid.* **11** (2013) 024] [arXiv:0903.1126] [INSPIRE].

[218] E. Gardi, E. Laenen, G. Stavenga and C.D. White, *Webs in multiparton scattering using the replica trick*, *JHEP* **11** (2010) 155 [arXiv:1008.0098] [INSPIRE].

[219] V. Del Duca et al., *The infrared structure of gauge theory amplitudes in the high-energy limit*, *JHEP* **12** (2011) 021 [arXiv:1109.3581] [INSPIRE].

[220] E. Gardi and C.D. White, *General properties of multiparton webs: Proofs from combinatorics*, *JHEP* **03** (2011) 079 [arXiv:1102.0756] [INSPIRE].

[221] E. Gardi, J.M. Smillie and C.D. White, *On the renormalization of multiparton webs*, *JHEP* **09** (2011) 114 [arXiv:1108.1357] [INSPIRE].

[222] V. Del Duca et al., *An infrared approach to Reggeization*, *Phys. Rev. D* **85** (2012) 071104 [arXiv:1108.5947] [INSPIRE].

[223] V. Ahrens, M. Neubert and L. Vernazza, *Structure of Infrared Singularities of Gauge-Theory Amplitudes at Three and Four Loops*, *JHEP* **09** (2012) 138 [arXiv:1208.4847] [INSPIRE].

[224] V. Del Duca, G. Falcioni, L. Magnea and L. Vernazza, *High-energy QCD amplitudes at two loops and beyond*, *Phys. Lett. B* **732** (2014) 233 [arXiv:1311.0304] [INSPIRE].

[225] S. Caron-Huot, *When does the gluon reggeize?*, *JHEP* **05** (2015) 093 [arXiv:1309.6521] [INSPIRE].

[226] E. Gardi, *From Webs to Polylogarithms*, *JHEP* **04** (2014) 044 [arXiv:1310.5268] [INSPIRE].

JHEP09(2024)072

[227] E. Gardi, J.M. Smillie and C.D. White, *The Non-Abelian Exponentiation theorem for multiple Wilson lines*, *JHEP* **06** (2013) 088 [arXiv:1304.7040] [INSPIRE].

[228] G. Falcioni et al., *Multiple Gluon Exchange Webs*, *JHEP* **10** (2014) 010 [arXiv:1407.3477] [INSPIRE].

[229] T. Becher and M. Neubert, *Infrared singularities of scattering amplitudes and N^3LL resummation for n-jet processes*, *JHEP* **01** (2020) 025 [arXiv:1908.11379] [INSPIRE].

[230] J.M. Henn and B. Mistlberger, *Four-Gluon Scattering at Three Loops, Infrared Structure, and the Regge Limit*, *Phys. Rev. Lett.* **117** (2016) 171601 [arXiv:1608.00850] [INSPIRE].

[231] A.J. Buras, M. Jamin, M.E. Lautenbacher and P.H. Weisz, *Effective Hamiltonians for $\Delta S = 1$ and $\Delta B = 1$ nonleptonic decays beyond the leading logarithmic approximation*, *Nucl. Phys. B* **370** (1992) 69 [*Addendum ibid.* **375** (1992) 501] [INSPIRE].

[232] H. Chen, I. Moult and H.X. Zhu, *Quantum Interference in Jet Substructure from Spinning Gluons*, *Phys. Rev. Lett.* **126** (2021) 112003 [arXiv:2011.02492] [INSPIRE].

[233] H. Chen, I. Moult and H.X. Zhu, *Spinning gluons from the QCD light-ray OPE*, *JHEP* **08** (2022) 233 [arXiv:2104.00009] [INSPIRE].

[234] X.L. Li, X. Liu, F. Yuan and H.X. Zhu, *Illuminating nucleon-gluon interference via calorimetric asymmetry*, *Phys. Rev. D* **108** (2023) L091502 [arXiv:2308.10942] [INSPIRE].

[235] Z. Nagy, *Three jet cross-sections in hadron hadron collisions at next-to-leading order*, *Phys. Rev. Lett.* **88** (2002) 122003 [hep-ph/0110315] [INSPIRE].

[236] Z. Nagy, *Next-to-leading order calculation of three jet observables in hadron hadron collision*, *Phys. Rev. D* **68** (2003) 094002 [hep-ph/0307268] [INSPIRE].

[237] M. Cacciari, G.P. Salam and G. Soyez, *The anti-k_t jet clustering algorithm*, *JHEP* **04** (2008) 063 [arXiv:0802.1189] [INSPIRE].

[238] J. Butterworth et al., *PDF4LHC recommendations for LHC Run II*, *J. Phys. G* **43** (2016) 023001 [arXiv:1510.03865] [INSPIRE].

[239] M.A. Ebert et al., *Subleading power rapidity divergences and power corrections for q_T*, *JHEP* **04** (2019) 123 [arXiv:1812.08189] [INSPIRE].

[240] G. Ferrera, W.-L. Ju and M. Schönherr, *Zero-bin subtraction and the q_T spectrum beyond leading power*, *JHEP* **04** (2024) 005 [arXiv:2312.14911] [INSPIRE].

[241] I. Moult, G. Vita and K. Yan, *Subleading power resummation of rapidity logarithms: the energy-energy correlator in $\mathcal{N} = 4$ SYM*, *JHEP* **07** (2020) 005 [arXiv:1912.02188] [INSPIRE].

[242] H. Chen, X. Zhou and H.X. Zhu, *Power corrections to energy flow correlations from large spin perturbation*, *JHEP* **10** (2023) 132 [arXiv:2301.03616] [INSPIRE].

[243] B. Agarwal et al., *Five-parton scattering in QCD at two loops*, *Phys. Rev. D* **109** (2024) 094025 [arXiv:2311.09870] [INSPIRE].

[244] G. De Laurentis, H. Ita, M. Klinkert and V. Sotnikov, *Double-virtual NNLO QCD corrections for five-parton scattering. I. The gluon channel*, *Phys. Rev. D* **109** (2024) 094023 [arXiv:2311.10086] [INSPIRE].

[245] G. De Laurentis, H. Ita and V. Sotnikov, *Double-virtual NNLO QCD corrections for five-parton scattering. II. The quark channels*, *Phys. Rev. D* **109** (2024) 094024 [arXiv:2311.18752] [INSPIRE].

JHEP09(2024)072

[246] Y.L. Dokshitzer, G. Marchesini and B.R. Webber, *Nonperturbative effects in the energy energy correlation*, *JHEP* **07** (1999) 012 [hep-ph/9905339] [INSPIRE].

[247] R. Fiore, A. Quartarolo and L. Trentadue, *Energy-energy correlation for Theta → 180-degrees at LEP*, *Phys. Lett. B* **294** (1992) 431 [INSPIRE].

[248] D. de Florian and M. Grazzini, *The Back-to-back region in e^+e^- energy-energy correlation*, *Nucl. Phys. B* **704** (2005) 387 [hep-ph/0407241] [INSPIRE].

[249] H.-M. Chang, M. Procura, J. Thaler and W.J. Waalewijn, *Calculating Track-Based Observables for the LHC*, *Phys. Rev. Lett.* **111** (2013) 102002 [arXiv:1303.6637] [INSPIRE].

[250] H.-M. Chang, M. Procura, J. Thaler and W.J. Waalewijn, *Calculating Track Thrust with Track Functions*, *Phys. Rev. D* **88** (2013) 034030 [arXiv:1306.6630] [INSPIRE].

[251] Y. Li et al., *Extending Precision Perturbative QCD with Track Functions*, *Phys. Rev. Lett.* **128** (2022) 182001 [arXiv:2108.01674] [INSPIRE].

[252] M. Jaarsma et al., *Renormalization group flows for track function moments*, *JHEP* **06** (2022) 139 [arXiv:2201.05166] [INSPIRE].

[253] H. Chen et al., *Multi-collinear splitting kernels for track function evolution*, *JHEP* **07** (2023) 185 [arXiv:2210.10058] [INSPIRE].

[254] H. Chen et al., *Collinear Parton Dynamics Beyond DGLAP*, arXiv:2210.10061 [INSPIRE].

[255] O.V. Tarasov, A.A. Vladimirov and A.Y. Zharkov, *The Gell-Mann-Low Function of QCD in the Three Loop Approximation*, *Phys. Lett. B* **93** (1980) 429 [INSPIRE].

[256] S.A. Larin and J.A.M. Vermaseren, *The three loop QCD Beta function and anomalous dimensions*, *Phys. Lett. B* **303** (1993) 334 [hep-ph/9302208] [INSPIRE].

[257] S. Moch, J.A.M. Vermaseren and A. Vogt, *The three loop splitting functions in QCD: The nonsinglet case*, *Nucl. Phys. B* **688** (2004) 101 [hep-ph/0403192] [INSPIRE].

[258] S. Moch, J.A.M. Vermaseren and A. Vogt, *The quark form-factor at higher orders*, *JHEP* **08** (2005) 049 [hep-ph/0507039] [INSPIRE].

[259] S. Moch, J.A.M. Vermaseren and A. Vogt, *Three-loop results for quark and gluon form-factors*, *Phys. Lett. B* **625** (2005) 245 [hep-ph/0508055] [INSPIRE].

[260] A. Idilbi, X.-D. Ji, J.-P. Ma and F. Yuan, *Threshold resummation for Higgs production in effective field theory*, *Phys. Rev. D* **73** (2006) 077501 [hep-ph/0509294] [INSPIRE].

[261] A. Idilbi, X.-D. Ji and F. Yuan, *Resummation of threshold logarithms in effective field theory for DIS, Drell-Yan and Higgs production*, *Nucl. Phys. B* **753** (2006) 42 [hep-ph/0605068] [INSPIRE].

[262] T. Becher, M. Neubert and B.D. Pecjak, *Factorization and Momentum-Space Resummation in Deep-Inelastic Scattering*, *JHEP* **01** (2007) 076 [hep-ph/0607228] [INSPIRE].

JHEP09(2024)072